Negative-Ion Photoelectron Spectroscopy, Gas-Phase Acidity, and Thermochemistry of the Peroxyl Radicals CH 3 OO and CH 3 CH 2 OO

ARTICLE *in* JOURNAL OF THE AMERICAN CHEMICAL SOCIETY · NOVEMBER 2001

Impact Factor: 12.11 · DOI: 10.1021/ja010942j · Source: PubMed

9 AUTHORS, INCLUDING:

Mark R Nimlos
National Renewable Energy Laboratory
167 PUBLICATIONS **5,190** CITATIONS
SEE PROFILE

Shuji Kato
Toho University
80 PUBLICATIONS **1,364** CITATIONS
SEE PROFILE

Mitchio Okumura
California Institute of Technology
133 PUBLICATIONS **3,028** CITATIONS
SEE PROFILE

Negative-Ion Photoelectron Spectroscopy, Gas-Phase Acidity, and Thermochemistry of the Peroxyl Radicals CH_3OO and CH_3CH_2OO

Stephen J. Blanksby,[†] Tanya M. Ramond,[‡] Gustavo E. Davico,[†,‡,||] Mark R. Nimlos,[†,§] Shuji Kato,[†] Veronica M. Bierbaum,*[,†] W. Carl Lineberger,*[,†,‡] G. Barney Ellison,*[,†] and Mitchio Okumura*[,⊥]

Department of Chemistry and Biochemistry, University of Colorado, Boulder, Colorado 80309-0215, JILA, University of Colorado and National Institute of Standards and Technology, Boulder, Colorado 80309-0440, National Renewable Energy Laboratory, Golden, Colorado 80401-3393, and Department of Chemistry, California Institute of Technology, Pasadena, California 91125

Received April 12, 2001

Abstract: Methyl, methyl-d_3, and ethyl hydroperoxide anions (CH_3OO^-, CD_3OO^-, and $CH_3CH_2OO^-$) have been prepared by deprotonation of their respective hydroperoxides in a stream of helium buffer gas. Photodetachment with 364 nm (3.408 eV) radiation was used to measure the adiabatic electron affinities: $EA[CH_3OO, \tilde{X}\ ^2A'']$ = 1.161 ± 0.005 eV, $EA[CD_3OO, \tilde{X}\ ^2A'']$ = 1.154 ± 0.004 eV, and $EA[CH_3CH_2OO, \tilde{X}\ ^2A'']$ = 1.186 ± 0.004 eV. The photoelectron spectra yield values for the term energies: $\Delta E(\tilde{X}\ ^2A''-\tilde{A}\ ^2A')[CH_3OO]$ = 0.914 ± 0.005 eV, $\Delta E(\tilde{X}\ ^2A''-\tilde{A}\ ^2A')[CD_3OO]$ = 0.913 ± 0.004 eV, and $\Delta E(\tilde{X}\ ^2A''-\tilde{A}\ ^2A')[CH_3CH_2OO]$ = 0.938 ± 0.004 eV. A localized RO−O stretching mode was observed near 1100 cm^{-1} for the ground state of all three radicals, and low-frequency R−O−O bending modes are also reported. Proton-transfer kinetics of the hydroperoxides have been measured in a tandem flowing afterglow−selected ion flow tube (FA-SIFT) to determine the gas-phase acidity of the parent hydroperoxides: $\Delta_{acid}G_{298}(CH_3OOH)$ = 367.6 ± 0.7 kcal mol^{-1}, $\Delta_{acid}G_{298}(CD_3OOH)$ = 367.9 ± 0.9 kcal mol^{-1}, and $\Delta_{acid}G_{298}(CH_3CH_2OOH)$ = 363.9 ± 2.0 kcal mol^{-1}. From these acidities we have derived the enthalpies of deprotonation: $\Delta_{acid}H_{298}(CH_3OOH)$ = 374.6 ± 1.0 kcal mol^{-1}, $\Delta_{acid}H_{298}(CD_3OOH)$ = 374.9 ± 1.1 kcal mol^{-1}, and $\Delta_{acid}H_{298}(CH_3CH_2OOH)$ = 371.0 ± 2.2 kcal mol^{-1}. Use of the negative-ion acidity/*EA* cycle provides the ROO−H bond enthalpies: $DH_{298}(CH_3OO-H)$ = 87.8 ± 1.0 kcal mol^{-1}, $DH_{298}(CD_3OO-H)$ = 87.9 ± 1.1 kcal mol^{-1}, and $DH_{298}(CH_3CH_2OO-H)$ = 84.8 ± 2.2 kcal mol^{-1}. We review the thermochemistry of the peroxyl radicals, CH_3OO and CH_3CH_2OO. Using experimental bond enthalpies, DH_{298}(ROO−H), and CBS/APNO ab initio electronic structure calculations for the energies of the corresponding hydroperoxides, we derive the heats of formation of the peroxyl radicals. The "electron affinity/acidity/CBS" cycle yields $\Delta_fH_{298}[CH_3OO]$ = 4.8 ± 1.2 kcal mol^{-1} and $\Delta_fH_{298}[CH_3CH_2OO]$ = −6.8 ± 2.3 kcal mol^{-1}.

Introduction

Alkyl peroxyl radicals (ROO) are generally the first oxidation products of saturated hydrocarbons in the troposphere.[1−3] Atmospheric hydrocarbons react with strong oxidizers such as HO, O_3, or NO_3. The HO radical reacts with saturated hydrocarbons by H atom abstraction.[2] The nascent alkyl radical, R, combines rapidly with atmospheric O_2 in a three-body reaction to produce the corresponding alkyl peroxyl radical.[1]

$$RH + OH \rightarrow R + H_2O \quad (1)$$

$$R + O_2 + M \rightarrow ROO + M \quad (2)$$

Atmospheric peroxyl radicals react quickly with NO to generate NO_2, which is photodissociated by sunlight to produce NO and O (^{3}P). The latter is primarily responsible for the formation of tropospheric ozone (reactions 3−5).[4,5] Given that NO and hydrocarbons are both byproducts of combustion, reactions 1−5 form a crucial part of the chemistry responsible for the formation of photochemical smog in industrialized areas.

$$ROO + NO \rightarrow RO + NO_2 \quad (3)$$

$$NO_2 + \text{sunlight} \rightarrow NO + O\ (^3P) \quad (4)$$

$$O_2 + O\ (^3P) + M \rightarrow O_3 + M \quad (5)$$

Alkyl peroxides are also known to play a role in the chemistry of combustion.[6] Under some conditions, particularly at low

* To whom correspondence should be addressed. E-mail: veronica.bierbaum@colorado.edu, wcl@jila.colorado.edu, barney@jila.colorado.edu, mo@its.caltech.edu.
† University of Colorado.
‡ JILA.
§ National Renewable Energy Laboratory.
⊥ California Institute of Technology.
|| Current address: Department of Chemistry, University of Idaho, Moscow, ID 83844-2343.

(1) Lightfoot, P. D.; Cox, R. A.; Crowley, J. N.; Destriau, M.; Hayman, G. D.; Jenkin, M. E.; Moortgat, G. K.; Zabel, F. *Atmos. Environ.* **1992**, *26A*, 1805.
(2) Madronich, S.; Greenberg, J.; Paulson, S. In *Atmospheric Chemistry and Global Change*, 1st ed.; Brasseur, G. P., Orlando, J. J., Tyndall, G. S., Eds.; Oxford University Press: New York, 1999; p 325.
(3) Le Bras, G. In *Chemical Processes in Atmospheric Oxidation*; Le Bras, G., Ed.; Springer: Berlin, 1997; Vol. 3, p 13.
(4) Finlayson-Pitts, B. J.; Pitts, J. N., Jr. *Science* **1997**, *276*, 1045.
(5) Kirchner, F.; Stockwell, W. R. *J. Geophys. Res.* **1996**, *101*, 21007.
(6) Benson, S. W. *J. Am. Chem. Soc.* **1965**, *87*, 972.

10.1021/ja010942j CCC: $20.00
Published on Web 09/07/2001

combustion temperatures (<700 K), hydrocarbon fuels can undergo a series of facile radical reactions involving the intermediacy of alkyl peroxyl radicals. In an internal combustion engine such chemistry may result in accelerated ignition and indeed premature ignition. This phenomenon is referred to as autoignition or "engine knock" and has practical ramifications for engine wear and efficiency.[7]

$$RCH_2{-}CH_3 + O_2 \xrightarrow{\Delta} RCH_2{-}CH_2 + HO_2 \quad (6)$$

$$RCH_2{-}CH_2 + O_2 \rightarrow RCH_2{-}CH_2OO \rightarrow RCH{=}CH_2 + HOO \quad (7)$$

The importance of alkyl peroxyl radicals in atmospheric and combustion processes has generated continued interest in the prototypical gas-phase reaction of ethyl radical with dioxygen (reaction 8). The experimental and theoretical data reported thus far have been summarized by Rienstra-Kiracofe et al.,[8] who used ab initio electronic structure calculations to investigate mechanisms for the formation of ethylene, acetaldehyde, and oxirane as products of this reaction. All of these channels involve the intermediacy of the ethyl peroxyl radical.

$$CH_3CH_2 + O_2 \rightarrow [CH_3{-}CH_2OO]^* \quad (8)$$

$$[CH_3{-}CH_2OO]^* \rightarrow CH_2{=}CH_2 + OOH \quad (9)$$

$$[CH_3{-}CH_2OO]^* \rightarrow CH_3CHO + OH \quad (10)$$

$$[CH_3{-}CH_2OO]^* \rightarrow c\text{-}CH_2CH_2O + OH \quad (11)$$

If the mechanisms of such reactions can be fully understood, it should be possible to extrapolate them to other, more complex hydrocarbon systems. However, even for this simple model system, crucial issues remain unresolved. In particular, the precise thermochemistry of reaction 8 is still disputed, with theorists[8,9] and experimentalists[10−13] differing by several kilocalories per mole on the magnitude of the resulting exothermicity.

In this article we describe the measurement of the negative-ion photoelectron spectra of the CH_3OO^-, CD_3OO^-, and $CH_3CH_2OO^-$ anions. Analysis of the kinetic energy of the

$$ROO^- + \hbar\omega_{364\ nm} \rightarrow ROO + e^-(KE) \quad (12)$$

scattered photoelectrons (KE) enables determination of the electron affinity (*EA*) of the corresponding peroxyl radical, *EA*(ROO). In addition to the photoelectron spectra, we have studied the proton-transfer kinetics of the corresponding hydroperoxides in a tandem flowing afterglow−selected ion flow tube (FA-SIFT). The proton-transfer kinetics establish the gas-

$$XH + ROO^- \rightleftarrows ROO{-}H + X^- \quad (13)$$

phase acidities of the hydroperoxides, $\Delta_{acid}G_{298}$(ROO−H). Bond enthalpies of the hydroperoxides [DH_{298}(ROO−H)] are obtained from the peroxyl radical electron affinities [*EA*(ROO)] and the enthalpy of deprotonation of the corresponding hydroperoxides [$\Delta_{acid}H_{298}$(ROO−H)].

There have been numerous studies of electronic properties of alkyl peroxyl radicals.[1,3,8,14] We can use generalized valence bond (GVB) diagrams[14−16] to represent the peroxide anions, ROO^-, the peroxyl radicals, ROO, and the peroxyl cations, ROO^+.

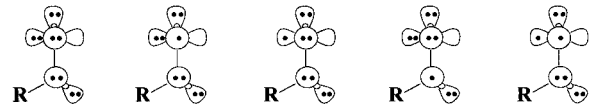

ROO^- ROO ROO^* ROO^* ROO^+ (14)

$\tilde{X}\,^1A'$ ≅ -1 eV $\tilde{X}\,^2A''$ ≡ 0 eV $\tilde{A}\,^2A'$ ≅ 1 eV $\tilde{B}\,^2A''$ ≅ 5 eV $\tilde{X}\,^3A''$ ≅ 11 eV

The ground electronic state of alkyl peroxyl radicals is ROO $\tilde{X}\,^2A''$. These radicals display two characteristic electronic excited states: a low-lying ROO $\tilde{A}\,^2A'$ state is present at about 1 eV, and there is a high-lying, dissociative state ROO $\tilde{B}\,^2A''$ at a term value of roughly 5 eV. The binding energy[14] of the alkyl peroxide anions, ROO^- $\tilde{X}\,^1A'$, is about 1 eV; ionization energies[17] of peroxyl radicals are high [*IP*(ROO) ≅ 11 eV]. The GVB representations depict the HOMO and HOMO-1 of ROO^- to be localized on the terminal oxygen. Therefore, detachment from these orbitals is expected to excite RO−O stretching modes in forming both the ground state and first excited states of the neutral.

Experiment

A. Preparation of Alkyl Hydroperoxides. Methyl hydroperoxide was prepared by methylation of hydrogen peroxide (Fisher Scientific) with dimethyl sulfate (Aldrich) in the presence of potassium hydroxide (Fisher Scientific), according to the literature procedure.[18,19] Methyl-d_3 hydroperoxide was prepared in the same way except that dimethyl-d_6 sulfate (Aldrich) was used in place of the unlabeled reagent. Ethyl hydroperoxide was prepared by a procedure analogous to that used for the methyl homologue except diethyl sulfate (Aldrich) was used and a 20-fold increase in reaction time was allowed. *tert*-Butyl hydroperoxide was obtained as a commercial sample (Aldrich). Care was taken in the preparation and handling of all peroxides, as these are known to be thermally unstable species and explosions have been reported by researchers in other laboratories.[18−20]

B. Negative-Ion Photoelectron Detachment. The 364 nm photoelectron spectra of CH_3OO^-, CD_3OO^-, and $CH_3CH_2OO^-$ were measured with a photoelectron spectrometer that has previously been described in detail.[21,22] The anions were prepared by reaction of the parent alkyl hydroperoxide with hydroxide ions in approximately

(7) Westbrook, C. K. *Chem. Ind. (London)* **1992**, *100*, 562.
(8) Rienstra-Kiracofe, J. C.; Allen, W. D.; Schaefer, H. F., III. *J. Phys. Chem.* **2000**, *104*, 9823.
(9) Brinck, T.; Lee, H.-N.; Jonsson, M. *J. Phys. Chem.* **1999**, *103*, 7094.
(10) Slagle, I. R.; Gutman, D. *J. Am. Chem. Soc.* **1985**, *107*, 5342.
(11) Slagle, I. R.; Ratajczak, E.; Gutman, D. *J. Phys. Chem.* **1986**, *90*, 402.
(12) Knyazev, V. D.; Slagle, I. R. *J. Phys. Chem.* **1998**, *102*, 1770.
(13) Wagner, A. F.; Slagle, I. R.; Sarzynski, D.; Gutman, D. *J. Phys. Chem.* **1990**, *94*, 1853.
(14) Clifford, E. P.; Wenthold, P. G.; Gareyev, R.; Lineberger, W. C.; DePuy, C. H.; Bierbaum, V. M.; Ellison, G. B. *J. Chem. Phys.* **1998**, *109*, 10293.
(15) Goddard, W. A., III; Harding, L. B. *Annu. Rev. Phys. Chem.* **1978**, *29*, 363.
(16) Bair, R. A.; Goddard, W. A., III. *J. Am. Chem. Soc.* **1982**, *104*, 2719.
(17) Litorja, M.; Ruscic, B. *J. Electron Spectrosc. Relat. Phenom.* **1998**, *97*, 131.
(18) Vaghjiani, G. L.; Ravishankara, A. R. *J. Phys. Chem.* **1989**, *93*, 1948.
(19) Criegee, R. In *Methoden der Organischen Chemie*; Houben, J., Weyl, T., Eds.; G. Thieme: Stuttgart, 1952; Vol. VII, p 6.
(20) Shanley, E. S. In *Organic Peroxides*, 1st ed.; Swern, D., Ed.; Wiley-Interscience: New York, 1972; Vol. 3, p 341.
(21) Leopold, D. G.; Murray, K. K.; Stevens-Miller, A. E.; Lineberger, W. C. *J. Chem. Phys.* **1985**, *83*, 4849.
(22) Ervin, K. M.; Lineberger, W. C. In *Gas-Phase Ion Chemistry*; Adams, N. G., Babcock, L. M., Eds.; JAI: Greenwich, CT, 1992; Vol. 1, p 121.

0.5 Torr of helium in the flowing afterglow ion source. Collisional relaxation with the helium buffer gas served to equilibrate the anions to a vibrational temperature of approximately 300 K. Further cooling to roughly 200 K was achieved by enclosing the flow tube in a jacket of liquid nitrogen. Anions were mass-selected using a Wien velocity filter and subsequently decelerated into an interaction region where the ion beam intersects at right angles with a photon beam from a fixed-frequency ($\lambda_0 = 363.8$ nm, 3.408 eV) CW argon ion laser in a buildup cavity, yielding approximately 100 W of circulating power. Photoelectrons were collected in a direction perpendicular to the plane of the ion beam−laser interaction and passed through a hemispherical energy analyzer onto a position-sensitive detector. The spectra were recorded as a function of electron kinetic energy (eKE), which is readily converted to electron binding energy (eBE) by subtracting the eKE from the laser photon energy. The absolute energy scale was fixed by the position of the $^3P_2 \leftarrow {}^2P_{3/2}$ transition in the O^- photoelectron spectrum. An additional small (<1%) energy compression factor was applied as determined from the comparison of the photoelectron spectrum of the tungsten ion (W^-) with known transitions in tungsten atom.[23]

Given the resolution of the instrument (±0.005 eV or 40 cm^{-1}), rotational bands cannot be resolved. Consequently, the exact peak positions are rotationally uncertain. To assign the exact position of the 0_0^0 transition, and thus assign the *EA*, it is necessary to apply a rotational correction. Let us suppose that the target anions have a mean rotational energy, ϵ''_{rot}, where ϵ''_{rot} is the Maxwell−Boltzmann average of the ion distribution, $\epsilon''_{rot} = \langle E''_{rot} \rangle$. Consequently, the measured, uncorrected peak position *EA* is simply

$$\text{uncorrected } EA = EA - \epsilon''_{rot} + \epsilon'_{rot} = EA + \Delta_{rot} \qquad (15)$$

where $\epsilon'_{rot} = \langle E'_{rot} \rangle$ is the Maxwell−Boltzmann average of the neutral distribution. Engelking[24] has derived useful, approximate expressions for the rotational correction, Δ_{rot}. In his expressions, k_B is the Boltzmann constant, *T* is the "effective" temperature of the ion beam, and *A*, *B*, and *C* are the rotational constants of the initial anion (″ state) and final neutral (′ state). For an asymmetric rotor, he obtains a rotational correction

$$\Delta_{rot} = k_B T\left[\frac{A'}{2A''} + \frac{B'}{2B''} + \frac{C'}{2C''} - \frac{3}{2}\right] + \frac{(B'' - B')}{3} \qquad (16)$$

Using this approach, the rotational corrections applied in this study are ≤0.002 eV.

The angular distribution of photoelectrons, $I(\theta)$, is given by the expression[25]

$$I(\theta) = \frac{\bar{\sigma}}{4\pi}[1 + \beta(E)P_2(\cos\theta)] \qquad (17)$$

where θ is the angle between the laser electric field vector and the electron collection direction, $\bar{\sigma}$ is the average photodetachment cross section, $P_2(\cos\theta) = 1/2(3\cos^2\theta - 1)$, and $\beta(E)$ is the anisotropy factor that depends on the energy of the photoelectron, *E*. The polarization of the incident laser beam, θ, can be varied by rotating a half-wave plate in the laser beam path. The photoelectron spectra shown here (Figures 1−3) were collected under conditions where θ was set to the magic angle of 54.7° such that $P_2(\cos\theta) = 0$ and therefore $I(\theta) = \bar{\sigma}/4\pi$ and is independent of β. Photoelectron spectra were also obtained at the laser polarization angles 0° and 90°. We then determined the asymmetry parameter, β, from the expression

$$\beta = \frac{I_{0°} - I_{90°}}{\frac{1}{2}I_{0°} + I_{90°}} \qquad (18)$$

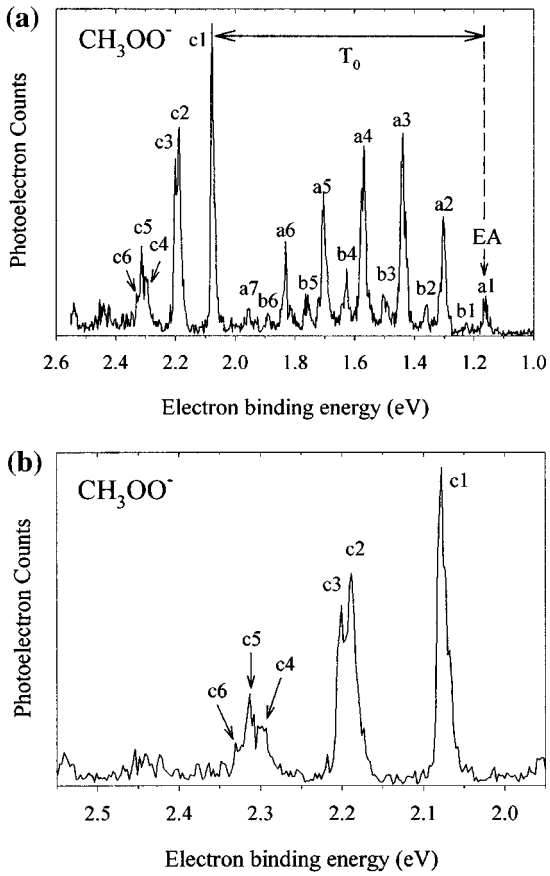

Figure 1. (a) 364 nm photoelectron spectrum of CH_3OO^- taken at 200 K and the magic angle polarization ($\theta = 54.7°$). (b) An expansion of the $\tilde{A} \leftarrow \tilde{X}$ transition spectral profile.

where $-1 \le \beta \le 2$. For molecules, detaching an electron from a π-like orbital yields $\beta < 0$, while an electron originating from a σ-like orbital gives an angular distribution of photoelectrons with $\beta > 0$. In this way, angular distribution information in photoelectron spectra can be used to distinguish between transitions to different electronic states.[26]

Spectra were measured at both 200 and 300 K (room temperature) vibrational temperature and compared in order to identify transitions that originate from vibrationally excited states in the anion. This allows for a secure assignment of the 0_0^0 peak.

C. Flowing Afterglow−Selected Ion Flow Tube Measurements. The gas-phase acidities of CH_3OOH, CD_3OOH, CH_3CH_2OOH, and $(CH_3)_3COOH$ were measured using a tandem flowing afterglow−selected ion flow tube (FA-SIFT) apparatus that has been previously described.[27] The acidity of the parent hydroperoxide was established by measurement of the rate constant for proton transfer between ROOH and a conjugate base of a reference acid, as well as the rate constant for the reverse reaction.[28] Measurements were conducted at 298 K.

$$ROO^- + XH \rightleftarrows ROOH + X^- \qquad (19)$$

The ratio of the two measured rate constants, k_{19} and k_{-19}, gives the proton-transfer equilibrium constant $K_{equi(19)}$, which is related to the difference in gas-phase acidities of ROOH and XH by a simple expression. If the acidity of the reference acid is known, $\Delta_{acid}G_T(HX)$, then the acidity of the target alkyl peroxide, can be extracted from eq 20.

(23) Moore, C. E. *Atomic Energy Levels*; National Bureau of Standards (U.S.): Washington, D.C., 1952.
(24) Engelking, P. C. *J. Phys. Chem.* **1986**, *90*, 4544.
(25) Cooper, J.; Zare, R. *J. Chem. Phys.* **1968**, *48*, 942.
(26) Schwartz, R. L.; Davico, G. E.; Ramond, T. M.; Lineberger, W. C. *J. Phys. Chem.* **1999**, *103*, 8213.
(27) Van Doren, J. M.; Barlow, S. E.; DePuy, C. H.; Bierbaum, V. M. *Int. J. Mass Spectrom. Ion Processes* **1987**, *81*, 85.
(28) Robinson, M. S.; Polak, M. K.; Bierbaum, V. M.; DePuy, C. H.; Lineberger, W. C. *J. Am. Chem. Soc.* **1995**, *117*, 6766.

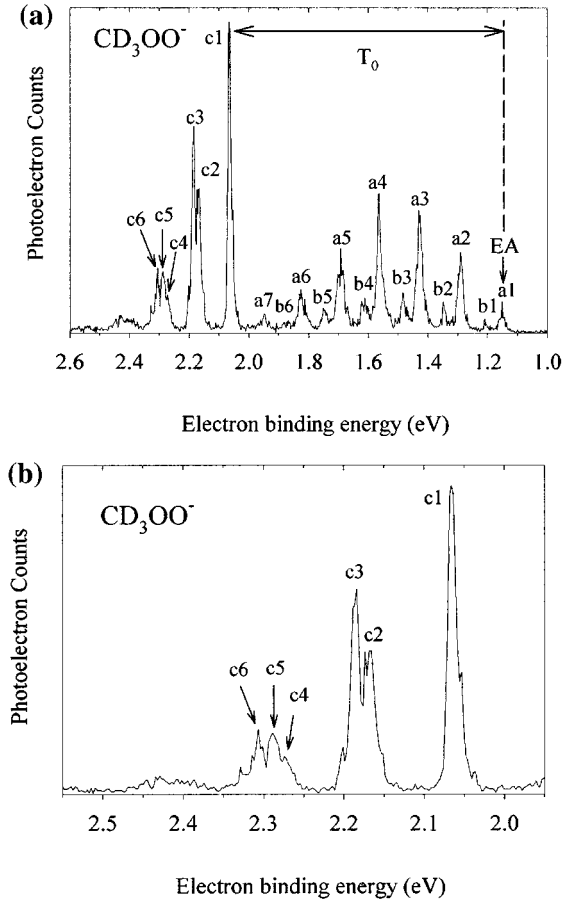

Figure 2. (a) 364 nm photoelectron spectrum of CD_3OO^- taken at 200 K and the magic angle polarization ($\theta = 54.7°$). (b) An expansion of the $\tilde{A} \leftarrow \tilde{X}$ transition spectral profile.

$$\Delta_{acid}G_T(\mathrm{ROOH}) - \Delta_{acid}G_T(\mathrm{HX}) = \Delta\Delta_{acid}G_T = RT \ln K_{equi(19)} \quad (20)$$

All rate constants reported in this article are presented with their associated statistical uncertainty along with other errors (e.g., mass discrimination and sample contamination). It should be noted that these uncertainties do not include systematic errors due to temperature, flow rates, and pressure measurements. Systematic errors of this kind will be the same for the measurement of forward and reverse rate constants and therefore need not be considered in the determination of K_{equi} and its associated uncertainty. However, the overall uncertainty for any given rate constant will typically be ±20%, where statistical and other errors (e.g., mass discrimination and sample contamination) are smaller than 20%.

The peroxide anions, ROO^- [where R = CH_3, CD_3, C_2H_5, and $(CH_3)_3C$], were prepared by the reaction of ROOH with a gas-phase base such as hydroxide ion, as previously reported.[29,30] Care was taken to minimize the contact of the alkyl hydroperoxides with metal prior to their introduction into the instrument,[31] and all lines were passivated for several minutes before measurements were undertaken. Reference acids were acetylene (HC≡CH, Matheson) and phenylacetylene (C_6H_5C≡CH, Aldrich). These reagents were used without further purification, with the exception of acetylene, which was passed through a stainless steel coil cooled to −78 °C in a dry ice/acetone bath to remove trace acetone from the sample.[32]

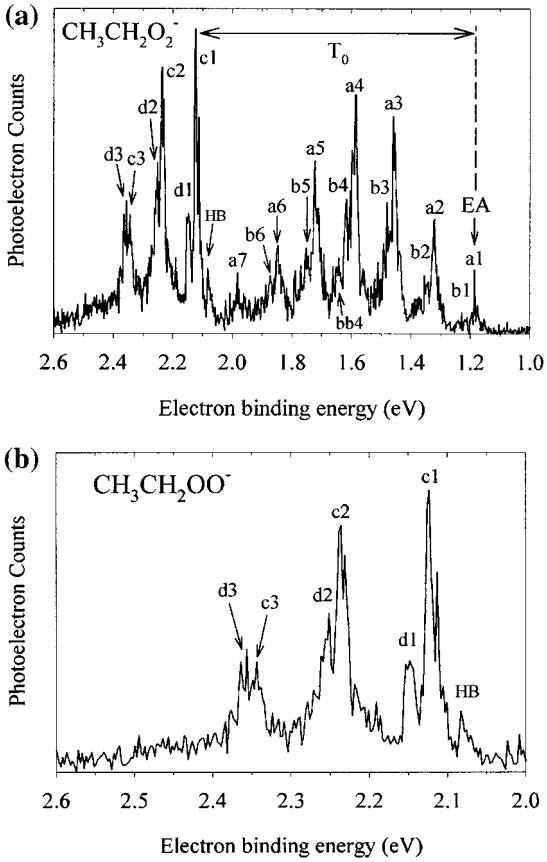

Figure 3. (a) 364 nm photoelectron spectrum of $CH_3CH_2OO^-$ taken at 200 K and the magic angle polarization ($\theta = 54.7°$). (b) An expansion of the $\tilde{A} \leftarrow \tilde{X}$ transition spectral profile.

D. Ab Initio Electronic Structure Calculations. Two different theoretical methods, both of which are available within the GAUSSIAN98 program package,[33] were used to investigate different aspects of the alkyl hydroperoxides. The first approach was the Becke 3LYP hybrid density functional method,[34] employed in conjunction with a correlation-consistent Dunning basis set of double-ζ quality (aug-cc-pVDZ)[35] to calculate optimized molecular structures, rotational constants, and harmonic frequencies (these data are available as Supporting Information). Harmonic frequencies and rotational constants calculated using this approach were employed in statistical thermodynamics calculations to derive the entropy and heat capacities of relevant species. The second approach used the Complete Basis Set (CBS)[36,37] method to determine thermodynamic properties of the alkyl hydroperoxides and the alkyl peroxyl radicals. The CBS/APNO approach, which has a reported uncertainty of 0.7 kcal mol^{-1}, was adopted for calculation of ROOH and ROO (where R = H, CH_3, CH_3CH_2). The less demanding

(29) Aschi, M.; Attina, M.; Cacace, F.; Cipollini, R.; Pepi, F. *Inorg. Chim. Acta* **1998**, *275*−*276*, 192.
(30) Schalley, C. A.; Schroeder, D.; Schwarz, H.; Moebus, K.; Boche, G. *Chem. Ber./Recl.* **1997**, *130*, 1085.
(31) Schalley, C. A.; Wesendrup, R.; Schroeder, D.; Weiske, T.; Schwarz, H. *J. Am. Chem. Soc.* **1995**, *117*, 7711.
(32) Perin, D. D.; Armarego, W. L. F.; Perrin, D. R. *Purification of Laboratory Chemicals*, 2nd ed.; Pergamon Press: Oxford, 1980.
(33) Frisch, M. J.; Trucks, G. W.; Schlegel, H. B.; Scuseria, G. E.; Robb, M. A.; Cheeseman, J. R.; Zakrzewski, V. G.; Montgomery, J. A., Jr.; Stratmann, R. E.; Burant, J. C.; Dapprich, S.; Millam, J. M.; Daniels, A. D.; Kudin, K. N.; Strain, M. C.; Farkas, O.; Tomasi, J.; Barone, V.; Cossi, M.; Cammi, R.; Mennucci, B.; Pomelli, C.; Adamo, C.; Clifford, S.; Ochterski, J.; Petersson, G. A.; Ayala, P. Y.; Cui, Q.; Morokuma, K.; Malick, D. K.; Rabuck, A. D.; Raghavachari, K.; Foresman, J. B.; Cioslowski, J.; Ortiz, J. V.; Baboul, A. G.; Stefanov, B. B.; Liu, G.; Liashenko, A.; Piskorz, P.; Komaromi, I.; Gomperts, R.; Martin, R. L.; Fox, D. J.; Keith, T.; Al-Laham, M. A.; Peng, C. Y.; Nanayakkara, A.; Gonzalez, C.; Challacombe, M.; Gill, P. M. W.; Johnson, B.; Chen, W.; Wong, M. W.; Andres, J. L.; Gonzalez, C.; Head-Gordon, M.; Replogle, E. S.; Pople, J. A. *Gaussian 98*, A.7; Gaussian Inc.: Pittsburgh, PA, 1998.
(34) Becke, A. D. *J. Phys. Chem.* **1993**, *98*, 5648.
(35) Dunning, T. H., Jr. *J. Chem. Phys.* **1989**, *90*, 1007.
(36) Montgomery, J. A.; Ochterski, J. W.; Petersson, G. A. *J. Chem. Phys.* **1994**, *101*, 5900.
(37) Ochterski, J. W.; Petersson, G. A.; Montgomery, J. A. *J. Chem. Phys.* **1996**, *104*, 2598.

Table 1. Data Extracted from the Photoelectron Spectra (Figures 1−3) of CH_3OO^-, CD_3OO^-, and $CH_3CH_2OO^-$ [a]

	EA (eV)	T_0 (eV)	β	ω_p (cm^{-1})	x_{pp} (cm^{-1})	ν (cm^{-1})	ν (cm^{-1})
CH_3OO $\tilde{X}$	1.161(5)		−0.7(2)	1147(3)	12(1)	1124(5)	482(9)
CH_3OO $\tilde{A}$		0.914(5)	−0.2(2)			1005(10)	910(10)
CD_3OO $\tilde{X}$	1.154(4)			1142(5)	9(1)	1123(7)	440(7)
CD_3OO $\tilde{A}$		0.913(4)				975(10)	840(10)
CH_3CH_2OO $\tilde{X}$	1.186(4)		−0.2(2)	1096(10)	4(2)	1089(16)	234(9)
CH_3CH_2OO $\tilde{A}$		0.938(4)	−0.2(2)			900(15)	178(10)

[a] The data treatments utilized to extract these values and their associated uncertainties (given in parentheses) are discussed in the text. The fundamental frequencies (ν) are listed without mode assignments. These are also discussed in the text.

CBS-Q protocol, with a reported uncertainty of 1.2 kcal mol^{-1}, was adopted for the larger $(CH_3)_3COOH$ and $(CH_3)_3COO$ systems.

Results

A. Negative-Ion Photoelectron Detachment of CH_3OO^- and CD_3OO^-. The 200 K magic angle photoelectron spectrum of CH_3OO^- is presented in Figure 1, and the critical data extracted from this spectrum (and those of CD_3OO^- and $CH_3CH_2OO^-$) are listed in Table 1. Similar to the photoelectron spectra[14,38] of HOO^- and DOO^-, there are two peak profiles present in the spectrum, indicative of transitions to two electronic states of the peroxyl radical. The first band at lower electron binding energy represents a transition to the ground state of the neutral radical, CH_3OO $\tilde{X}$ $^2A''$, while the second band at higher eBE represents a transition to the first excited state of the neutral radical, CH_3OO $\tilde{A}$ $^2A'$. Peak **c1** (Figure 1) is unambiguously assigned as the 0_0^0 of the $\tilde{A} \leftarrow \tilde{X}$ transition. If feature **a1** is assigned as the electron affinity, this yields an $EA[CH_3OO] = 1.161 \pm 0.005$ eV and a term energy $T_0(\tilde{X}\ CH_3OO - \tilde{A}\ CH_3OO)$ of 0.914 ± 0.005 eV (or 7370 ± 40 cm^{-1}). This measurement of the term energy $T_0(CH_3OO)$ is in excellent agreement with the recent cavity ring-down measurement reported by Pushkarsky et al.[39] of 7382.8 ± 0.5 cm^{-1} as well as the longstanding value of Hunziker and Wendt[40] of 7375 ± 6 cm^{-1}.

The 200 K magic angle photoelectron spectrum of CD_3OO^- is shown in Figure 2. An initial comparison does not show any great difference from that of CH_3OO^- in Figure 1, and the overall interpretation of the peaks parallels that of CH_3OO^-. The electron affinity is measured as $EA[CD_3OO] = 1.154 \pm 0.004$ eV, slightly less than that for CH_3OO. CD_3OO has a term energy, $T_0 = 0.913 \pm 0.004$ eV (7365 ± 30 cm^{-1}), which agrees with values of Pushkarsky et al. (7372.6 ± 0.5 cm^{-1}) and Hunziker and Wendt.[39,40]

The extended progression of peaks corresponding to the CH_3OO $\tilde{X} \leftarrow CH_3OO^-$ $\tilde{X}$ state transition (Figure 1) indicates a significant geometrical change between the ground-state anion and neutral structures. By contrast, the second Franck−Condon envelope of peaks corresponding to the $\tilde{A} \leftarrow \tilde{X}$ transition has a narrower profile, with the 0_0^0 (**c1**) peak being the most intense and subsequent peaks rapidly decreasing in intensity. This indicates a smaller relative change between the $\tilde{X}$ CH_3OO^- and $\tilde{A}$ CH_3OO geometries than that observed in the $\tilde{X} \leftarrow \tilde{X}$ transition. The anion and neutral structures predicted by both the qualitative GVB expression (eq 14) and B3LYP/aug-cc-pVDZ ab initio calculations support this explanation. In the $\tilde{X} \leftarrow \tilde{X}$ transition the O−O bond length is calculated to change by about 0.2 Å and the C−O−O bond angle by 5°. In contrast, the $\tilde{A} \leftarrow \tilde{X}$ transition calculations predict a change in the O−O bond length of roughly 0.1 Å and a change in the C−O−O bond angle of about 2° (see Supporting Information).

Table 2. Negative-Ion Photoelectron Peak Positions (rotationally uncorrected) for CH_3OO^- and CD_3OO^- [a]

$CH_3OO^- + \hbar\omega_{364} \rightarrow CH_3OO + e^-$ (KE)
$CH_3OO^- + \hbar\omega_{364} \rightarrow CD_3OO + e^-$ (KE)

for CH_3OO the fundamentals are: $\nu_p = 1124(5)$ cm^{-1} (O−O stretch), $\nu_q = 482(9)$ cm^{-1} (C−O−O bend), $\nu_s = 910(10)$ cm^{-1} (see text), $\nu_t = 1005(10)$ cm^{-1} (see text)

for CD_3OO the fundamentals are: $\nu_p = 1123(7)$ cm^{-1} (O−O stretch), $\nu_q = 440(7)$ cm^{-1} (C−O−O bend), $\nu_s = 840(10)$ cm^{-1} (see text), $\nu_t = 975(10)$ cm^{-1} (see text)

			CH_3OO	CD_3OO
$\tilde{X}$ $^2A''$	a1	0_0^0	0	0
	b1	q_0^1	515(15)	470(15)
	a2	p_0^1	1125(15)	1130(10)
	b2	$p_0^1q_0^1$	1600(15)	1565(10)
	a3	p_0^2	2225(15)	2235(10)
	b3	$p_0^2q_0^1$	2700(20)	2660(10)
	a4	p_0^3	3290(15)	3310(10)
	b4	$p_0^3q_0^1$	3750(15)	3750(10)
	a5	p_0^4	4365(15)	4380(10)
	b5	$p_0^4q_0^1$	4810(20)	4820(15)
	a6	p_0^5	5390(15)	5425(10)
	b6	$p_0^5q_0^1$	5870(15)	5850(20)
	a7	p_0^6	6390(15)	6490(25)
$\tilde{A}$ $^2A'$	c1	0_0^0	0	0
	c2	s_0^1	910(10)	840(10)
	c3	t_0^1	1005(10)	975(10)
	c4	s_0^2	1790(10)	1690(15)
	c5	$s_0^1t_0^1$	1910(10)	1800(10)
	c6	t_0^2	2040(15)	1950(10)

[a] Uncertainties are given in parentheses. Peak positions are given in wavenumbers (cm^{-1}) relative to 0_0^0 transitions (peaks **a1** and **c1**). Assignments are given for the most prominent transitions labeled as indicated in Figures 1 and 2.

In the Franck−Condon profile for detachment to the ground state, CH_3OO $\tilde{X}$ $^2A''$, there are two series of features. The most prominent progression is denoted by peaks **a1**−**a7** in Figure 1. The peak **a1** is assigned as the 0_0^0 transition, while peaks **a2**−**a7** correspond to a progression of six quanta ($\upsilon_p = 1-6$) of an active mode which we label **p**. The measured energy spacings (Table 2) between the peaks in this progression (**a1**−**a2**, **a1**−**a3**, **a1**−**a4**, etc.) correspond to the fundamental $[G(1)-G(0)]$ and overtones $[G(\upsilon_p)-G(0)$, where $\upsilon_p = 2-6]$ of mode **p** and can be fitted to eq 21[41] using a weighted least-squares approach.

$$G(\upsilon_p) - G(0) = \omega_p(\upsilon_p + 1/2) - x_{pp}(\upsilon_p + 1/2)^2 - 1/2\omega_p + 1/4x_{pp} \quad (21)$$

(38) Ramond, T. M.; Davico, G. E.; Schwartz, R. L.; Lineberger, W. C., manuscript in preparation, 2001.
(39) Pushkarsky, M. B.; Zalyubovsky, S. J.; Miller, T. A. *J. Chem. Phys.* **2000**, *112*, 10695.
(40) Hunziker, H. E.; Wendt, H. R. *J. Chem. Phys.* **1976**, *64*, 3488.

Fitting these data to eq 21 gives the harmonic frequency of mode **p**, $\omega_p = 1147 \pm 3$ cm^{-1}, and an anharmonicity term, $x_{pp} = 12 \pm 1$ cm^{-1}. Using these parameters, we can precisely extract a value for the $1 \leftarrow 0$ vibrational transition of mode **p**, $\nu_p = 1124 \pm 5$ cm^{-1}. In addition to the primary progression, a less intense although clearly resolved second progression is identified in peaks **b1**−**b6**. These peaks appear to the higher binding energy side of the **a** peaks and may be identified as a combination band with this series. We assign **b1**−**b6** as a combination of the progression due to mode **p**, discussed above, plus one quantum of a mode we have labeled **q**. Taking a weighted average of these energy spacings (Table 2), we obtain the fundamental of mode **q** to be $\nu_q = 482 \pm 9$ cm^{-1}.

For the ground state of CD_3OO, the **a** peaks (Table 2) allow us to determine a harmonic frequency, $\omega_p = 1142 \pm 5$ cm^{-1}, and an anharmonicity, $x_{pp} = 9 \pm 1$ cm^{-1}. Using these parameters, we can precisely extract a value for the fundamental of mode **p**, $\nu_p = 1123 \pm 7$ cm^{-1}. The **b** series of peaks is again a combination of the progression due to mode **p** plus one quantum of mode **q**. Taking a weighted average of these energy spacings (Table 2), we obtain the fundamental of mode **q** to be $\nu_q = 440 \pm 7$ cm^{-1}.

For ground-state CH_3OO, the fundamental of the primary progression, $\nu_p = 1124 \pm 5$ cm^{-1}, appears to correlate well with other fundamental O−O vibrational transitions in peroxyl radicals: (i) for HOO, $\nu_3 = 1097.63$ cm^{-1} as measured by Tuckett and co-workers,[42,43] (ii) for matrix-isolated CH_3OO, $\nu_6 = 1109$ cm^{-1} measured by Nandi et al.,[44] and (iii) for CH_3OO the ab initio harmonic frequency, $\omega_6 = 1149$ cm^{-1}, calculated at the B3LYP/aug-cc-pVDZ level of theory. From both the GVB diagrams (eq 14) and the ab initio geometries, one anticipates strong activity in the RO−O stretching mode upon detachment of the peroxide anion, ROO^-, to the $\tilde{X}$ state of the neutral. On the basis of these considerations and the good agreement between fundamental frequencies, we assign mode **p** to the CH_3O−O stretching mode 6. Similarly, the fundamental frequency $\nu_q = 482 \pm 9$ cm^{-1} correlates well with both the fundamental $\nu_8 = 492$ cm^{-1} measured by Nandi et al.[44] for matrix-isolated CH_3OO and the harmonic frequency $\omega_8 = 491$ cm^{-1}, calculated at the B3LYP/aug-cc-pVDZ level of theory, which corresponds to a H_3C−O−O bending mode. Theoretical geometries predict activity in the H_3C−O−O bending mode upon detachment of the peroxide anion, CH_3OO^-, to the $\tilde{X}$ state of the neutral radical. These considerations lead us to assign mode **q** to the H_3C−O−O bending mode 8.

These assignments are further supported by the spectrum of CD_3OO^-. The harmonic (ω_p) and fundamental (ν_p) frequencies of mode **p** extracted from the CD_3OO^- spectrum are very similar to those obtained from the CH_3OO^- spectrum, and both isotopomers also have similar anharmonicity in this mode. The magnitude of this value is also similar to that observed in the DOO^- photoelectron spectrum.[38] The fact that ω_p and fundamental ν_p do not change appreciably upon deuteration confirms the assignment of this mode to a localized O−O stretch; a mode that involves hydrogen motion would have been expected to shift to a lower frequency upon deuteration. This rationale is also consistent with the matrix work of Nandi et al., where the fundamental of the O−O stretch mode is largely unaffected by deuteration, shifting from 1109 ± 12 to 1144 ± 12 cm^{-1} in CH_3OO and CD_3OO.[44] In contrast, the frequency ν_q is shifted about 40 cm^{-1} lower upon deuteration, supporting the assignment of mode **q** to the C−O−O bend. Although the hydrogen atoms in this mode may not be moving with respect to the carbon, bending the carbon toward oxygen requires hydrogen motion. Therefore, one would anticipate such a shift to lower frequency. This shift is analogous to that observed in the matrix experiments.[44]

Examination of the Franck−Condon envelope for the CH_3OO $\tilde{A} \leftarrow CH_3OO^-$ $\tilde{X}$ transition (see expansion Figure 1b) reveals a progression of two active modes of similar intensity. Peak **c1** is assigned to the 0_0^0 transition, while the peaks **c2** and **c4** correspond to one and two quanta, respectively, of the mode which we designate **s**. The positions of peaks **c1** and **c2**, given in Table 2, fix the fundamental of mode **s** to be $\nu_s = 910 \pm 10$ cm^{-1}. The second progression in the excited state is represented by the peaks **c3** and **c6**, which correspond to one and two quanta, respectively, of the mode which we have assigned as **t**. The positions of peaks **c1** and **c2**, given in Table 2, fix the fundamental of mode **t** to be $\nu_t = 1005 \pm 10$ cm^{-1}. The peak **c5** in Figure 1 represents a combination band of one quantum of **s** and one quantum of **t**.

The $\tilde{A} \leftarrow \tilde{X}$ transition peaks show activity in two modes (**s** and **t)** of similar intensity and frequency. The fundamental frequency $\nu_s = 910 \pm 10$ cm^{-1} is comparable to the frequencies (i) $\nu_3 = 929.068$ cm^{-1}, which is the fundamental of the O−O stretching mode of the $\tilde{A}$ state of HOO measured by Tuckett and co-workers,[42,43] and (ii) the vibrational transition at 896 ± 9 cm^{-1} measured for the $\tilde{A}$ state of CH_3OO by Hunziker and Wendt.[40] The B3LYP/aug-cc-pVDZ calculated harmonic mode $\omega_7 = 917$ cm^{-1} is similar in magnitude to ν_s and corresponds to a "symmetric" C−O−O stretching mode. However, the magnitude of $\nu_t = 1005 \pm 10$ cm^{-1} is not significantly different from that of ν_s. The former frequency is similar in magnitude to the calculated harmonic frequency $\omega_6 = 1015$ cm^{-1}, which corresponds to a C−O−O "antisymmetric" stretching mode. The GVB diagrams and ab initio calculations both predict some activity in the CH_3O−O stretching vibration for the $\tilde{A} \leftarrow \tilde{X}$ transition. For this reason, it is not clear which of these two frequencies, if either, could be strictly assigned to an O−O stretch. Furthermore, the ab initio calculations suggest that the $\tilde{A}$ state vibrations in CH_3OO are unlike the local modes observed for the ground state, in that the normal modes involve a significant amount of mixing of local modes.

The CD_3OO^- spectrum also shows two active modes close in frequency and intensity. One quantum of the first mode is observed at the peak **c2** that appears 840 cm^{-1} from the 0_0^0 transition (**c1**), with a second quantum at 1690 cm^{-1} (**c4**). The second active mode appears at 975 cm^{-1} (**c3**), with a second quantum at 1950 cm^{-1} (**c6**). The peak **c5** at 1800 cm^{-1} corresponds to a combination band of one quantum of each of these modes. By analogy with the CH_3OO^- spectrum, we assign these two modes as **s** and **t** with fundamentals $\nu_s = 840 \pm 10$ cm^{-1} and $\nu_t = 975 \pm 10$ cm^{-1}. The value of ν_s is red-shifted by about 70 cm^{-1} compared with the corresponding frequency for CH_3OO. This indicates a significant hydrogen contribution to the motion of mode **s**, and therefore this mode cannot be assigned as a pure O−O stretch. By analogy to the $\tilde{X} \leftarrow \tilde{X}$ state assignments, and by comparison with the ab initio frequency motions discussed for CH_3OO, there is likely some C−O−O bend involved in the motion. The fundamental frequency ν_t has also shifted upon deuteration although somewhat less than in the case of ν_s. This suggests that H/D motion is a small

(41) Bernath, P. F. *Spectra of Atoms and Molecules*, 1st ed.; Oxford University Press: New York, 1995.

(42) Tuckett, R. P.; Freedman, P. A.; Jones, W. J. *Mol. Phys.* **1979**, *37*, 379.

(43) Tuckett, R. P.; Freedman, P. A.; Jones, W. J. *Mol. Phys.* **1979**, *37*, 403.

(44) Nandi, S.; Blanksby, S. J.; Zhang, X.; Nimlos, M.; Dayton, D.; Ellison, G. B. *J. Phys. Chem. A* **2001**, in press.

component of mode **t**, and thus it should be closer to a localized O−O stretch than mode **s**. Thus, we see evidence for mixing between local modes in the two normal modes observed in the $\tilde{A} \leftarrow \tilde{X}$ transition. On the basis of their intensity, both modes likely have a large component of O−O stretch with contributions from motion involving the hydrogen atoms, likely the C−O−O bend.

The asymmetry parameters β for both electronic transitions in CH_3OO^- are reported in Table 1. The $\tilde{X} \leftarrow \tilde{X}$ transition carries an average β of -0.7 ± 0.2, while the $\tilde{A} \leftarrow \tilde{X}$ transition has a β of -0.2 ± 0.2. These values agree well with the corresponding β values observed for HOO.[38] They are both negative, suggesting detachment from a π-like orbital. The detachment into the $\tilde{X}$ state is close to a β of -1, which implies that the detected electrons are ejected from an essentially pure π orbital. Detachment into the $\tilde{A}$ state yields a β closer to 0, indicating that the orbital from which the electrons are detached possesses some of the σ character of the O−C bond.

B. Negative-Ion Photoelectron Detachment of $CH_3CH_2OO^-$. The 200 K magic angle photoelectron spectrum of $CH_3CH_2OO^-$ is displayed in Figure 3. The spectrum is more congested than that of CH_3OO^- or CD_3OO^-, as would be expected for a larger molecule with a greater number of modes. However, the overall structure remains remarkably similar. One sees the same peak intensity envelopes representing transitions into two electronic states of the neutral. The peak **c1** is assigned to the 0_0^0 feature of the $\tilde{A} \leftarrow \tilde{X}$ transition. Peak **a1** is the origin of the $\tilde{X} \leftarrow \tilde{X}$ transition and thus gives the electron affinity, $EA[CH_3CH_2OO] = 1.186 \pm 0.004$ eV, and the term energy, $T_0 = 0.938 \pm 0.004$ eV (7565 ± 30 cm^{-1}), in agreement with the earlier findings of Hunziker and Wendt (7593 ± 6 cm^{-1}).[40] The same primary ground-state progression observed in CH_3OO^- and CD_3OO^- appears in peaks **a1**−**a5**, and we assign the active mode responsible as **p**. Fitting the energy spacings (Table 3) to eq 21 as previously described gives the harmonic frequency, $\omega_p = 1096 \pm 10$ cm^{-1}, and a small anharmonicity, $x_{pp} = 4 \pm 2$ cm^{-1}. Using these parameters, we can extract the fundamental frequency of mode **p** to be $\nu_p = 1089 \pm 16$ cm^{-1}. A second progression, **b1**−**b6**, is assigned as a combination of the progression due to mode **p** plus one quantum of a mode we have labeled **u**. Taking a weighted average of these energy spacings (Table 3), we obtain the fundamental of mode **u** to be $\nu_u = 234 \pm 9$ cm^{-1}. This frequency is small enough that one would expect to observe a combination band involving two quanta of mode **u** on top of the **p** progression. This is supported by the observation of peak **bb4**; however, any other members of such a progression are obscured by noise in the data.

The similarity of ω_p and ν_p between CH_3OO, CD_3OO, and CH_3CH_2OO is evidence that this frequency corresponds to a local O−O stretching mode, as increasing the mass of the alkyl substituent has a minimal effect on the measured frequency. The fundamental frequency, $\nu_p = 1089 \pm 10$ cm^{-1}, for CH_3CH_2OO also correlates well with the O−O stretching frequencies: (i) $\nu_3 = 1097.63$ cm^{-1} measured[42,43] for HOO, (ii) $\nu_{15} = 1112$ cm^{-1} measured[45] for matrix-isolated CH_3CH_2OO, and (iii) $\omega_8 = 1199$ cm^{-1}, the calculated harmonic frequency that corresponds to a localized O−O stretching mode. On the basis of these considerations, we assign mode **p** to the CH_3CH_2O−O stretching mode 8.

The assignment of mode **u** is not assisted by matrix frequency data, as they cannot observe such low frequencies. However, analogy with the CH_3OO and CD_3OO radicals would identify **u** as a bending mode. Furthermore, the downward shift in the fundamental frequency from $\nu_q = 482 \pm 9$ cm^{-1} for CH_3OO to $\nu_u = 234 \pm 9$ cm^{-1} for CH_3CH_2OO supports this assignment. Moving the carbon toward the oxygen would involve movement of more atoms for CH_3CH_2OO than for CH_3OO. Calculations of the harmonic frequencies predict two a′ modes in this region: $\omega_{12} = 501$ cm^{-1}, which corresponds to the C−O−O bending mode (cf. CH_3OO), and $\omega_{13} = 305$ cm^{-1}, which corresponds to a C−C−O bending mode. Thus, the active mode **u** may be assigned as a bending mode, although precisely which atoms are involved remains undetermined.

Table 3. Negative-Ion Photoelectron Peak Positions (rotationally uncorrected) for $CH_3CH_2OO^-$ [a]

$CH_3CH_2OO^- + \bar{h}\omega_{364} \rightarrow CH_3CH_2OO + e^-$ (KE)

for CH_3CH_2OO the fundamentals are: $\nu_p = 1089(16)$ cm^{-1} (O−O stretch), $\nu_u = 234(9)$ cm^{-1} (bend), $\nu_s = 900(15)$ cm^{-1} (O−O stretch), $\nu_v = 178(10)$ cm^{-1} (bend)

$\tilde{X}\ ^2A''$	a1	0_0^0	0
	b1	u_0^1	240(15)
	a2	p_0^1	1100(10)
	b2	$p_0^1u_0^1$	1305(15)
	a3	p_0^2	2180(15)
	b3	$p_0^2u_0^1$	2315(15)
	a4	p_0^3	3245(15)
	b4	$p_0^3u_0^1$	3490(10)
	bb4	$p_0^3u_0^2$	3695(10)
	a5	p_0^4	4305(15)
	b5	$p_0^4u_0^1$	4545(15)
	a6	p_0^5	5330(15)
	b6	$p_0^5u_0^1$	5540(10)
	a7	p_0^6	6435(10)
$\tilde{A}\ ^2A'$	HB	*b*	−345(15)
	c1	0_0^0	0
	d1	v_0^1	190(10)
	c2	s_0^1	900(15)
	d2	$s_0^1v_0^1$	1050(15)
	c3	s_0^2	1785(15)
	d3	$s_0^2v_0^1$	1910(25)

[a] Peak positions are given in wavenumbers (cm^{-1}) relative to 0_0^0 transitions (peaks **a1** and **c1**). Assignments are given for the most prominent transitions labeled as indicated in Figure 3. [b] See text for details.

In the $\tilde{A} \leftarrow \tilde{X}$ transition, the largest progression is an active mode denoted by the series of peaks **c1**−**c3**. Peak **c1** is assigned to the 0_0^0 transition, while the peaks **c2** and **c3** correspond to one and two quanta, respectively, of the mode which we designate **s**. The energy spacing of the peaks **c1** and **c2** gives the fundamental frequency of this progression, $\nu_s = 900 \pm 15$ cm^{-1}. In addition, there is evidence of a second active mode in the less intense **d** series of peaks. These features appear to the higher binding energy side of the **s** progression and are thus are assigned as the **s** progression plus one quantum of mode **v**. A weighted average of these energy spacings gives the fundamental of mode **v** as $\nu_v = 178 \pm 10$ cm^{-1}. Finally, the peak labeled "HB" (Figure 3) to the lower binding energy side of peak **c1** is assigned as a hot band, as its intensity significantly decreases when the sample is cooled from 300 to 200 K.

By analogy with HOO and CH_3OO, and from examination of the GVB diagrams, activity in the O−O stretch is expected for detachment to the $^2A'$ electronic state. Thus, mode **s** is assigned as the O−O stretch. The fundamental frequency, $\nu_s = 900 \pm 15$ cm^{-1}, is comparable to the $\tilde{A}$ state vibrational transition for CH_3CH_2OO, measured to be 918 ± 9 cm^{-1} by Hunziker and Wendt.[40] In contrast to the $\tilde{A} \leftarrow \tilde{X}$ transition of

(45) Chettur, G.; Snelson, A. *J. Phys. Chem.* **1987**, *91*, 3483.

CH_3OO and CD_3OO, the second series of peaks corresponds to an active mode with a small fundamental frequency, $\nu_v = 178 \pm 10$ cm^{-1}. Thus, mode **v** is not expected to involve any significant O−O stretching character. The low frequency is more consistent with a bending motion. The lowest calculated harmonic frequency of a′ symmetry is $\omega_{13} = 279$ cm^{-1}, which corresponds to a C−O−O bending mode.

The β parameters for the two $CH_3CH_2OO^-$ electronic transitions are given in Table 1. The $\tilde{X} \leftarrow \tilde{X}$ and the $\tilde{A} \leftarrow \tilde{X}$ transitions have the same asymmetry, with a negative value of -0.2 ± 0.2. This finding is consistent with the other peroxide systems studied, where negative β parameters are also observed for both transitions.[14]

C. Gas-Phase Acidity. Acetylene ($\Delta_{acid}G_{298}[C_2H_2] = 370.3 \pm 0.3$ kcal mol^{-1}) was used as a reference acid[46−48] to establish the gas-phase acidities of methyl and methyl-d_3 hydroperoxides, by measuring the proton-transfer kinetics.

$$CH_3OO^- + HC{\equiv}CH \rightleftarrows CH_3OOH + HC{\equiv}C^- \quad (22)$$

$$CD_3OO^- + HC{\equiv}CH \rightleftarrows CD_3OOH + HC{\equiv}C^- \quad (23)$$

The reaction of the methyl peroxide anion with acetylene was found to give two product ions: (i) the acetylide ion, generated by proton transfer, and (ii) the $CH_3OO^-{\cdot}C_2H_2$ cluster ion. The overall reaction rate constant, $k_{overall} = 2.09 (\pm 0.13) \times 10^{-11}$ cm^3 molecule^{-1} s^{-1}, represents the measured rate of depletion of the reactant anion. This value is small, suggesting a slow, endothermic reaction. In such cases, the cluster is usually thought to form from ions in the low-energy fraction of the thermal ion population, while the higher energy fraction undergoes the proton transfer. Therefore, the overall rate ($k_{overall}$) is multiplied by the amount of proton-transfer product ions as a fraction of all product ions to give the rate of proton transfer, $k_{22} = 1.25 (\pm 0.38) \times 10^{-11}$ cm^3 molecule^{-1} s^{-1}. The stated uncertainty for this rate also takes into account mass discrimination effects involved in such a treatment. The reverse reaction of the acetylide ion with methyl hydroperoxide was found to proceed significantly more rapidly and to form no clusters. The exothermic reaction produces two major product ions: (i) the methyl peroxide anion was generated by proton transfer and (ii) the hydroxide anion was produced via an $E_{CO}2$ mechanism similar to that described by DePuy and co-workers for methyl nitrite (eq 24).[49,50]

$$CH_3OOH + HC{\equiv}C^- \rightarrow CH_2O + HO^- + HC{\equiv}CH \quad (24)$$

Electronic structure calculations show that these two reactions both proceed energetically below the entrance channel and may therefore be considered as directly competitive.[50] Thus, the overall uncorrected rate constant for acetylide ion depletion may be used for the rate of proton transfer, $k_{-22} = 5.62 (\pm 0.15) \times 10^{-10}$ cm^3 molecule^{-1} s^{-1}. However, the methyl hydroperoxide was contaminated with some diethyl ether resulting from incomplete separation during the synthetic preparation. Although diethyl ether does not react with acetylide,[51] it may decrease the measured concentration of methyl hydroperoxide and consequently give an artificially lower reaction rate. As a consequence, we used the measured rate constant as a lower limit for the true rate of proton transfer and utilized the calculated collision rate,[52] $k_{collision} = 3.0 \times 10^{-9}$ cm^3 molecule^{-1} s^{-1}, as an upper limit for this exothermic proton transfer. Combining these boundary rates with k_{22}, according to eq 20, gives a recommended value of $\Delta\Delta_{acid}G_{298} = -2.7 \pm 0.6$ kcal mol^{-1}, where the stated uncertainty includes both upper and lower bounds. Thus, the absolute gas-phase acidity of methyl hydroperoxide is $\Delta_{acid}G_{298}[CH_3OOH] = 367.6 \pm 0.7$ kcal mol^{-1}. Despite the conservative assignments of error limits, the final uncertainty for the gas-phase acidity is still pleasingly small.[53] An analogous treatment of the data for methyl-d_3 hydroperoxide gave the following rates for forward and reverse proton-transfer reactions: $k_{23} = 1.43 (\pm 0.45) \times 10^{-11}$ cm^3 molecule^{-1} s^{-1} and $k_{-23} = 2.65 (\pm 0.07) \times 10^{-10}$ cm^3 molecule^{-1} s^{-1} ($k_{collision} = 2.28 \times 10^{-9}$ cm^3 molecule^{-1} s^{-1}). Using these results, we recommend a value of $\Delta\Delta_{acid}G_{298} = -2.4 \pm 0.8$ kcal mol^{-1}, and thus the absolute gas-phase acidity is determined to be $\Delta_{acid}G_{298}[CD_3OOH] = 367.9 \pm 0.9$ kcal mol^{-1}.

We used phenyl acetylene ($\Delta_{acid}G_{298}[C_6H_5C{\equiv}CH] = 362.9 \pm 2.0$ kcal mol^{-1})[54] as a reference acid to establish the gas-phase acidity of ethyl hydroperoxide. Although the gas-phase acidity of hydrogen fluoride ($\Delta_{acid}G_{298}[HF] = 365.8 \pm 0.2$ kcal mol^{-1}) is more precisely known,[55−59] reactions of HF with $CH_3CH_2OO^-$ and F^- with CH_3CH_2OOH led to numerous reaction channels which obscured the proton-transfer kinetics.[50]

$$CH_3CH_2OO^- + C_6H_5C{\equiv}CH \rightleftarrows CH_3CH_2OOH + C_6H_5C{\equiv}C^- \quad (25)$$

The reaction of the ethyl peroxide anion with phenyl acetylene produces the phenyl acetylide anion exclusively. This proton transfer is rapid, with a rate constant of $k_{25} = 1.18 (\pm 0.06) \times 10^{-9}$ cm^3 molecule^{-1} s^{-1}, suggesting an exothermic reaction. The reverse reaction of the phenyl acetylide anion with ethyl hydroperoxide produced (i) the ethyl peroxide anion by proton

(46) Mordaunt, D. H.; Ashfold, M. N. R. *J. Chem. Phys.* **1994**, *101*, 2630.

(47) Ervin, K. M.; Gronert, S.; Barlow, S. E.; Gilles, M. K.; Harrison, A. G.; Bierbaum, V. M.; DePuy, C. H.; Linberger, W. C.; Ellison, G. B. *J. Am. Chem. Soc.* **1990**, *112*, 5750.

(48) The gas-phase acidity cited here is derived from the measured C−H bond dissociation energy in acetylene. While this bond dissociation energy agrees, within experimental uncertainty, with the value derived by Ervin et al., it is established with greater precision and is therefore adopted here. The values for entropy and heat capacity used in the calculation of the gas-phase acidity from the bond dissociation energy are tabulated by Ervin et al.

(49) King, G. K.; Maricq, M. M.; Bierbaum, V. M.; DePuy, C. H. *J. Am. Chem. Soc.* **1981**, *103*, 7133.

(50) Blanksby, S. J.; Kato, S.; Bierbaum, V. M.; Ellison, G. B., manuscript in preparation, 2001.

(51) No ethoxide ions ($CH_3CH_2O^-$) were detected in this reaction, suggesting that diethyl ether does not react with the acetylide ions under these conditions.

(52) Su, T.; Chesnavich, W. J. *J. Chem. Phys.* **1982**, *76*, 5183.

(53) A reviewer has expressed some concern regarding our method for deriving the forward rate constant for proton transfer (k_{22}). In our treatment, the cluster ions are excluded from the overall measured rate constant ($k_{overall}$) in order to derive the rate of the proton transfer. Although we believe this logic is sound, if we include the cluster ions and use simply the $k_{overall}$ for the rate of proton transfer, we calculate $\Delta\Delta_{acid}G_{298} = -2.4 \pm 0.4$ kcal mol^{-1}, which falls almost entirely within the stated uncertainty of our recommended value.

(54) Bartmess, J. E.; Scott, J. A.; McIver, R. T., Jr. *J. Am. Chem. Soc.* **1979**, *101*, 6047.

(55) The $\Delta_{acid}G_{298}$ value for HF can be calculated from the known heats of formation and entropies of HF, H^+, and F^- that are given here and are reported in the references indicated: $\Delta_fH_{298}[HF] = -65.320 \pm 0.167$ kcal mol^{-1}, $\Delta_fS_{298}[HF] = 41.5342 \pm 0.0007$ cal mol^{-1} K^{-1}, $\Delta_fH_{298}[F^-] = -59.456 \pm 0.072$ kcal mol^{-1}, $\Delta_fS_{298}[F^-] = 34.794 \pm 0.009$ cal mol^{-1} K^{-1}, $\Delta_fH_{298}[H^+] = 365.6828 \pm 0.0025$ kcal mol^{-1}, $\Delta_fS_{298}[H^+] = 26.040 \pm 0.009$ cal mol^{-1} K^{-1}.

(56) Cox, J. D., Wagman, D. D., Medvedev, V. A., Eds. *CODATA Key Values For Thermodynamics*; Hemisphere: New York, 1989.

(57) Chase, M. W., Jr. *J. Phys. Chem. Ref. Data, Monograph 9* **1998**, 1.

(58) *Handbook of Chemistry and Physics*, 73rd ed.; Lide, D. R., Ed.; CRC Press: Boca Raton, FL, 1992.

(59) Blondel, C.; Cacciani, P.; Delsart, C.; Trainham, R. *Phys. Rev. A* **1989**, *40*, 3698.

transfer and the secondary cluster ions, $CH_3CH_2OO^-\cdot(CH_3CH_2OOH)$ and $CH_3CH_2OO^-\cdot(CH_3CH_2OOH)_2$, and (ii) the hydroxide and acetaldehyde enolate anions by the $E_{CO}2$ mechanism previously discussed (cf. eq 24). The overall rate coefficient, $k_{overall} = 4.20\ (\pm 0.12) \times 10^{-10}$ cm^3 molecule^{-1} s^{-1}, is significantly smaller than that of the forward reaction, demonstrating that the reverse proton transfer is endothermic. For a slow endothermic reaction, it is unclear whether (i) the proton-transfer and $E_{CO}2$ reactions are directly competitive (cf. k_{-22}) or (ii) the proton-transfer and $E_{CO}2$ reactions arise from different energy fractions of the thermal ion population. Thus, there are two possible treatments of these data: (i) the overall reaction rate, $k_{overall}$, is taken to represent the proton-transfer rate k_{-25}, giving $\Delta\Delta_{acid}G_{298} = 0.61 \pm 0.03$ kcal mol^{-1}, or (ii) the overall rate is partitioned, based on the fraction of proton-transfer product ions, giving $k_{-25} = 1.77\ (\pm 0.88) \times 10^{-10}$ cm^3 molecule^{-1} s^{-1}, where the large uncertainty is due to mass discrimination effects. This gives $\Delta\Delta_{acid}G_{298} = 1.1 \pm 0.3$ kcal mol^{-1}. For such an endothermic reaction, neither scenario may be discounted, and we therefore recommend a difference in gas-phase acidities of $\Delta\Delta_{acid}G_{298} = 1.0 \pm 0.4$ kcal mol^{-1} to cover both possibilities. This gives a conservative gas-phase acidity of $\Delta_{acid}G_{298}(CH_3CH_2OOH) = 363.9 \pm 2.0$ kcal mol^{-1}. It is significant to note that the uncertainty due to the treatment of k_{-25} is almost completely absorbed by the large uncertainty in the gas-phase acidity of the reference acid, phenyl acetylene ($\Delta_{acid}G_{298}[C_6H_5C{\equiv}CH] = 362.9 \pm 2.0$ kcal mol^{-1}).

To make meaningful thermochemical comparisons between alkyl peroxides, the rates of proton transfer were measured under the same conditions for *tert*-butyl hydroperoxide with phenyl acetylene. In the absence of α-hydrogens on the *tert*-butyl hydroperoxide, the forward and reverse rate constants were only corrected for clustering reactions that are particularly prevalent for such a large system.

$$(CH_3)_3COO^- + C_6H_5C{\equiv}CH \rightleftarrows (CH_3)_3COOH + C_6H_5C{\equiv}C^- \quad (26)$$

These corrections yield the rates $k_{26} = 7.29\ (\pm 1.46) \times 10^{-10}$ cm^3 molecule^{-1} s^{-1} and $k_{-26} = 7.54\ (\pm 1.51) \times 10^{-10}$ cm^3 molecule^{-1} s^{-1}. The similarity between the rates suggests a nearly thermoneutral reaction with $\Delta\Delta_{acid}G_{298} = -0.02 \pm 0.17$ kcal mol^{-1}, such that $\Delta_{acid}G_{298}[(CH_3)_3COOH] = 362.9 \pm 2.0$ kcal mol^{-1}, in good agreement with the previously reported value[14] of $\Delta_{acid}G_{298}[(CH_3)_3COOH] = 363.2 \pm 2.0$ kcal mol^{-1} (we recommend the revised value for future reference). It is important, however, that this experiment fixes the difference in gas-phase acidity between ethyl and *tert*-butyl hydroperoxide to be 1.0 ± 0.4 kcal mol^{-1}.

D. Entropy and Enthalpy Calculations. One can extract bond energies from measured electron affinities and gas-phase acidities.[60] The simple thermochemical cycle in eq 27 combines (i) the enthalpy of deprotonation of the parent alkyl hydroperoxide ($\Delta_{acid}H_{298}$[ROOH]) with (ii) the electron affinity of the corresponding alkyl peroxyl radical (*EA*[ROO]) and (iii) the ionization potential of the hydrogen atom (*IP*[H]), yielding the ROO−H bond dissociation enthalpy (DH_{298}[ROO−H]) for the alkyl hydroperoxide.

The final term in this expression corresponds to the sum of the integrated heat capacities, which is always small (≤0.3 kcal mol^{-1}) and can therefore be ignored[60] in favor of the simplified expression

$$DH_{298}[ROO{-}H] = \Delta_{acid}H_{298}[ROOH] - IP[H] + EA[ROO] - \int_0^{298} dT(C_p[ROO] - C_p[ROO^-] + C_p[H] - C_p[H^+]) \quad (27)$$

$$DH_{298}[ROO{-}H] \cong \Delta_{acid}H_{298}[ROOH] - IP[H] + EA[ROO] \quad (28)$$

The $\Delta_{acid}H_{298}$[ROOH] term in eq 28 must be extracted from the experimentally determined $\Delta_{acid}G_{298}$ value and a calculated entropy of deprotonation, $\Delta_{acid}S_{298}$, via the simple relation $\Delta_{acid}H_{298} = \Delta_{acid}G_{298} + T\Delta_{acid}S_{298}$. Ab initio electronic structure calculations (Becke 3LYP hybrid density functional calculations) were employed to generate harmonic vibrational frequencies and rotational constants for the ROOH and ROO$^-$ species. These values are tabulated as Supporting Information and were used to estimate the entropies of these molecules using equilibrium statistical thermodynamics,[61,62] with rigid rotor and harmonic oscillator approximations. Clearly, when R = CH_3, CH_3CH_2, and $(CH_3)_3C$, both ROOH and ROO$^-$ species will possess low-energy internal rotors. For the most part, however, the contributions of the internal rotors to the entropy will be common to both ROOH and ROO$^-$ and will therefore cancel out in the calculation of $\Delta_{acid}S_{298}$. The exception to this is the internal rotation about the RO−OH axis in the alkyl hydroperoxides. In the absence of experimental rotational data for these species, a more rigorous treatment of the entropy to include an explicit treatment of the contributions of the RO−OH rotor would also include some approximations.[63,64] To allow for these problems involving internal rotors, we chose the very conservative uncertainty limits of ±2.3 cal mol^{-1} K^{-1} for our calculated $\Delta_{acid}S_{298}$ values. The following entropies of deprotonation were computed: $\Delta_{acid}S_{298}[CH_3OOH] = 23.3 \pm 2.3$ cal mol^{-1} K^{-1}, $\Delta_{acid}S_{298}[CD_3OOH] = 23.3 \pm 2.3$ cal mol^{-1} K^{-1}, $\Delta_{acid}S_{298}[CH_3CH_2OOH] = 23.8 \pm 2.3$ cal mol^{-1} K^{-1}, and $\Delta_{acid}S_{298}[(CH_3)_3COOH] = 24.5 \pm 2.3$ cal mol^{-1} K^{-1}. Use of these calculated entropies with the measured acidities provides the enthalpies of deprotonation: $\Delta_{acid}H_{298}[CH_3OOH] = 374.6 \pm 1.0$ kcal mol^{-1}, $\Delta_{acid}H_{298}[CD_3OOH] = 374.9 \pm 1.1$ kcal mol^{-1}, $\Delta_{acid}H_{298}[CH_3CH_2OOH] = 371.0 \pm 2.2$ kcal mol^{-1}, and $\Delta_{acid}H_{298}[(CH_3)_3COOH] = 370.2 \pm 2.1$ kcal mol^{-1}. Using the measured electron affinities of $EA[CH_3OO] = 26.8 \pm 0.1$ kcal mol^{-1}, $EA[CD_3OO] = 26.6 \pm 0.1$ kcal mol^{-1}, $EA[CH_3CH_2OO] = 27.3 \pm 0.1$ kcal mol^{-1}, and $EA[(CH_3)_3COO] = 27.6 \pm 0.3$ kcal mol^{-1} and the precisely known ionization potential of the hydrogen atom,[65] $IP[H] = 313.587\ 347 \pm 0.000\ 001$ kcal mol^{-1}, the bond dissociation enthalpies are calculated, via eq 28, to be $DH_{298}[CH_3OO{-}H] = 87.8 \pm 1.0$ kcal mol^{-1}, $DH_{298}[CD_3OO{-}H] = 87.9 \pm 1.1$ kcal mol^{-1}, $DH_{298}[CH_3CH_2OO{-}H] = 84.8 \pm 2.2$ kcal mol^{-1}, and $DH_{298}[(CH_3)_3COO{-}H] = 84.2 \pm 2.1$ kcal mol^{-1}. By making a small correction for the difference in heat capacities at 298 K (see eq

(60) Berkowitz, J.; Ellison, G. B.; Gutman, D. *J. Phys. Chem.* **1994**, *98*, 2745.

(61) Davico, G. E.; Bierbaum, V. M.; DePuy, C. H.; Ellison, G. B.; Squires, R. R. *J. Am. Chem. Soc.* **1995**, *117*, 2590.

(62) Herzberg, G. *Infrared and Raman Spectra of Polyatomic Molecules*; D. Van Nostrand Co.: New York, 1945.

(63) Given the potential problems arising from internal rotor contributions to $\Delta_{acid}S_{298}$, we checked our harmonic oscillator−rigid rotor $\Delta_{acid}S_{298}$ values against those calculated using the software package of Hodgson and McKinnon. The latter approach separates S_{vib} from S_{introt} and calculates each explicitly. This calculation gives $\Delta_{acid}S_{298}$ (CH_3OOH) = 23.0 cal mol^{-1} K^{-1} and $\Delta_{acid}S_{298}$ (CH_3CH_2OOH) = 23.6 cal mol^{-1} K^{-1}, which differ from our harmonic oscillator−rigid rotor values (Table 4) by <0.5 cal mol^{-1} K^{-1}, which is within the stated uncertainty.

(64) Hodgson, D. W.; McKinnon, J. T., manuscript in preparation, 2001.

(65) Moore, C. *Atomic Energy Levels*; National Bureau of Standards: Washington, D.C., 1971.

29), it is possible to calculate the bond enthalpy at the 0 K limit which is, by definition, the bond dissociation energy.[60,66]

$$D_0[\mathrm{ROO-H}] = DH_{298}[\mathrm{ROO-H}] - \int_0^{298} \mathrm{d}T(C_p[\mathrm{ROO}] - C_p[\mathrm{ROOH}] + C_p[\mathrm{H}]) \quad (29)$$

The heat capacities C_p[ROOH], C_p[ROO], and C_p[H] can be estimated[61,62] using calculated data. Such calculations give $D_0[CH_3OO-H] = 86.9 \pm 1.0$ kcal mol^{-1}, $D_0[CD_3OO-H] = 87.0 \pm 1.1$ kcal mol^{-1}, $D_0[CH_3CH_2OO-H] = 83.9 \pm 2.2$ kcal mol^{-1}, and $D_0[(CH_3)_3COO-H] = 83.3 \pm 2.1$ kcal mol^{-1}.

Discussion

A. Thermochemistry. The thermochemical parameters that have been determined in this study for CH_3OO and CH_3CH_2OO and the corresponding hydroperoxides are listed in Table 4. These data are augmented with values previously measured for the HOO and $(CH_3)_3COO$ radicals. Bond enthalpies calculated using Complete Basis Set[36,37] ab initio electronic structure methods appear as a footnote to Table 4. The experimentally derived bond enthalpies, DH_{298}[ROO−H], presented above give rise to the possibility of determining accurate heats of formation for the corresponding peroxyl radicals, $\Delta_f H_{298}$[ROO], by the simple relationship:

$$\Delta_f H_{298}[\mathrm{ROO}] = DH_{298}[\mathrm{ROO-H}] + \Delta_f H_{298}[\mathrm{ROOH}] - \Delta_f H_{298}[\mathrm{H}] \quad (30)$$

However, to extract the heat of formation of the ROO radical in this way, the heat of formation of the parent hydroperoxide, $\Delta_f H_{298}$[ROOH], is required. The available literature values are collected in Table 5, but selecting a single reliable heat of formation for either CH_3OOH or CH_3CH_2OOH proves difficult, as neither has been precisely measured. Two problems are identified that make these compounds difficult to study experimentally: (i) the difficulty in obtaining pure compounds, and (ii) the instability of these small alkyl hydroperoxides, which have a susceptibility to heterogeneous decomposition on metal and glass surfaces.[67]

The only experimental data in the literature[68,69] appear to be $\Delta_f H_{298}[CH_3OOH] = -31.3$ kcal mol^{-1} (for which no uncertainty is specified) and $\Delta_f H_{298}[CH_3CH_2OOH] = -45 \pm 12$ kcal mol^{-1}. The earliest estimates in the literature are those derived by Benson and co-workers[67,70] utilizing the group additivity (GA) scheme,[71,72] based on the experimentally measured heats of formation for the dialkyl peroxides and hydrogen peroxide. The most recent group additivity values give $\Delta_f H_{298}[CH_3OOH] = -31.4 \pm 1.0$ kcal mol^{-1} and $\Delta_f H_{298}[CH_3CH_2OOH] = -39.4 \pm 1.0$ kcal mol^{-1}, where the confidence limits are estimated by comparing GA values with the experimental data[73] available for HOOH and $(CH_3)_3COOH$ (Table 5). Benassi et al. have calculated the heats of formation using molecular mechanics and low-level ab initio methods.[74] Employing an atom equivalents scheme, they recommend the values $\Delta_f H_{298}[CH_3OOH] = -33$ kcal mol^{-1} and $\Delta_f H_{298}[CH_3CH_2OOH] = -40$ kcal mol^{-1}. Lay et al. have attempted to evaluate the available thermodynamic data to obtain a best estimate for the heat of formation of methyl hydroperoxide.[75] They use the heat of formation of methyl peroxyl radical determined by Slagle and Gutman[10] from experimental data and an estimated "average bond energy" for the O−H bond in ROOH compounds[76] of 88.2 ± 0.4 kcal mol^{-1} to derive $\Delta_f H_{298}[CH_3OOH] = -33.4 \pm 1.2$ kcal mol^{-1}. This value is combined with data from isodesmic reaction calculations to give a computed value for the heat of formation of ethyl hydroper-

Table 4. Thermochemical Parameters Determined for the Peroxyl Radicals ROO and Their Corresponding Hydroperoxide Species ROOH, where R = H, CH_3, CD_3, CH_3CH_2, and $(CH_3)_3C$

		ref
HOO		
EA ($\tilde{X}\ ^2A''$ HOO)/eV	1.076 ± 0.006	14, 38, 79
$\Delta E(\tilde{X}\ ^2A''-\tilde{A}\ ^2A')$[HOO]/eV	0.871 ± 0.007	14, 38
$\Delta_{acid}G_{298}$(HOOH)/kcal mol^{-1}	369.7 ± 0.8	derived from values below
$\Delta_{acid}H_{298}$(HOOH)/kcal mol^{-1}	376.4 ± 0.8	derived (eq 28)
$\Delta_{acid}S_{298}$(HOOH)/cal mol^{-1} K^{-1}	23.5	80
DH_{298}(HOO−H)/kcal mol^{-1}	87.9 ± 0.8[a]	17
D_0(HOO−H)/kcal mol^{-1}	86.7 ± 0.8	17
CH_3OO		
EA($\tilde{X}\ ^2A''$ CH_3OO)/eV	1.161 ± 0.005	this work
$\Delta E(\tilde{X}\ ^2A''-\tilde{A}\ ^2A')$[$CH_3OO$]/eV	0.914 ± 0.005	this work
$\Delta_{acid}G_{298}$(CH_3OOH)/kcal mol^{-1}	367.6 ± 0.7	this work
$\Delta_{acid}H_{298}$(CH_3OOH)/kcal mol^{-1}	374.6 ± 1.0	this work
$\Delta_{acid}S_{298}$(CH_3OOH)/cal mol^{-1} K^{-1}	23.3 ± 2.3	this work
DH_{298}(CH_3OO−H)/kcal mol^{-1}	87.8 ± 1.0[a]	this work
D_0(CH_3OO−H)/kcal mol^{-1}	86.9 ± 1.0	this work
CD_3OO		
EA($\tilde{X}\ ^2A''$ CD_3OO)/eV	1.154 ± 0.004	this work
$\Delta E(\tilde{X}\ ^2A''-\tilde{A}\ ^2A')$[$CD_3OO$]/eV	0.913 ± 0.004	this work
$\Delta_{acid}G_{298}$(CD_3OOH)/kcal mol^{-1}	367.9 ± 0.9	this work
$\Delta_{acid}H_{298}$(CD_3OOH)/kcal mol^{-1}	374.9 ± 1.1	this work
$\Delta_{acid}S_{298}$(CD_3OOH)/cal mol^{-1} K^{-1}	23.3 ± 2.3	this work
DH_{298}(CD_3OO−H)/kcal mol^{-1}	87.9 ± 1.1	this work
D_0(CD_3OO−H)/kcal mol^{-1}	87.0 ± 1.1	this work
C_2H_5OO		
EA($\tilde{X}\ ^2A''$ C_2H_5OO)/eV	1.186 ± 0.004	this work
$\Delta E(\tilde{X}\ ^2A''-\tilde{A}\ ^2A')$[$C_2H_5OO$]/eV	0.938 ± 0.004	this work
$\Delta_{acid}G_{298}$(C_2H_5OOH)/kcal mol^{-1}	363.9 ± 2.0	this work
$\Delta_{acid}H_{298}$(C_2H_5OOH)/kcal mol^{-1}	371.0 ± 2.2	this work
$\Delta_{acid}S_{298}$(C_2H_5OOH)/cal mol^{-1} K^{-1}	23.8 ± 2.3	this work
DH_{298}(C_2H_5OO−H)/kcal mol^{-1}	84.8 ± 2.2[a]	this work
D_0(C_2H_5OO−H)/kcal mol^{-1}	83.9 ± 2.2	this work
$(CH_3)_3COO$		
EA($\tilde{X}\ ^2A''$ $(CH_3)_3COO$)/eV	1.196 ± 0.011	14
$\Delta E(\tilde{X}\ ^2A''-\tilde{A}\ ^2A')$[$(CH_3)_3COO$]/eV	0.967 ± 0.011	14
$\Delta_{acid}G_{298}$[$(CH_3)_3COOH$]/kcal mol^{-1}	362.9 ± 2.0	this work
$\Delta_{acid}H_{298}$[$(CH_3)_3COOH$]/kcal mol^{-1}	370.2 ± 2.1	this work
$\Delta_{acid}S_{298}$[$(CH_3)_3COOH$]/cal mol^{-1} K^{-1}	24.5 ± 2.3	this work
DH_{298}[$(CH_3)_3COO$−H]/kcal mol^{-1}	84.2 ± 2.1[a]	this work
D_0[$(CH_3)_3COO$−H]/kcal mol^{-1}	83.3 ± 2.1	this work

[a] CBS/APNO calculations give the following bond enthalpies for comparison with our experimental values: DH_{298}(HOO−H) = 86.7 ± 0.7 kcal mol^{-1}, DH_{298}(CH_3OO−H) = 85.1 ± 0.7 kcal mol^{-1}, and DH_{298}(C_2H_5OO−H) = 84.9 ± 0.7 kcal mol^{-1}. CBS-Q calculations give DH_{298}[$(CH_3)_3COO$−H] = 83.6 ± 1.2 kcal mol^{-1}.

(66) Ervin, K. M. *Chem. Rev.* **2001**, *101*, 391.
(67) Benson, S. W. *J. Chem. Phys.* **1964**, *40*, 1007.
(68) Khursan, S. L.; Martem'yanov, V. S. *Russ. J. Phys. Chem. (Engl. Trans.)* **1991**, *65*, 321.
(69) Stathis, E. C.; Egerton, A. C. *Trans. Faraday. Soc.* **1940**, *36*, 606.
(70) Benson, S. W.; Shaw, R. In *Organic Peroxides*; Swern, D., Ed.; Wiley-Interscience: New York, 1970; Vol. 1, p 105.
(71) Benson, S. W.; Cruickshank, F. R.; Golden, D. M.; Haugen, H. E.; O'Neal, H. E.; Rodgers, A. S.; Shaw, R.; Walsh, R. *Chem. Rev.* **1969**, *69*, 279.
(72) Benson, S. W. *Thermochemical Kinetics*, 2nd ed.; Wiley-Interscience: New York, 1976.
(73) Benson, S. W.; Cohen, N. In *Peroxyl Radicals*; Alfassi, Z., Ed.; Wiley: Chichester, 1997; p 49.
(74) Benassi, R.; Folli, U.; Sbardellati, S.; Taddei, F. *J. Comput. Chem.* **1993**, *14*, 379.
(75) Lay, T. H.; Krasnoperov, L. N.; Venanzi, C. A.; Bozzelli, J. W.; Shokhirev, N. V. *J. Phys. Chem.* **1996**, *100*, 8240.

Table 5. Comparison of the Available Literature Heats of Formation (kcal mol^{-1}) for ROO and ROOH with Those Determined in This Study, where R = H, CH_3, CH_3CH_2, $(CH_3)_3C$

Δ_fH_{298}[HOO]	3.0 ± 0.4	$OH + ClO \rightleftarrows HOO + Cl$[81,82]
	3.3 ± 0.8	IE(HOO) and AE(HOO^+/HOOH)[17]
	3.5 ± 0.5	group additivity[73]
	2.9 ± 0.7	CBS/APNO calculation
	3.3 ± 0.9	negative-ion/acidity/CBS[a]
Δ_fH_{298}[HOOH]	-32.48 ± 0.05	calorimetry[80]
	-32.5 ± 1.0	group additivity[73]
	-31.7 ± 0.7	CBS/APNO calculation
Δ_fH_{298}[CH_3OO]	2.7 ± 0.8	$CH_3 + O_2 \rightleftarrows CH_3OO$[10]
	2.9 ± 1.5	$CH_3 + O_2 \rightleftarrows CH_3OO$[83]
	2.2 ± 1.2	$CH_3 + O_2 \rightleftarrows CH_3OO$[12]
	5.5 ± 1.0	$Br + CH_3OOH \rightleftarrows CH_3OO + HBr$[84] tied to DH_{298}[CH_3OO-H] = 88.5 ± 0.5 kcal mol^{-1} and Δ_fH_{298}[CH_3OOH] = 30.9 ± 1.0 kcal mol^{-1}
	5.2 ± 1.1	group additivity using DH_{298}[CH_3OO-H] = 88.6 ± 0.5 kcal mol^{-1} [73]
	2.07 ± 0.7	CBS/APNO
	4.8 ± 1.2	negative-ion/acidity/CBS[a]
Δ_fH_{298}[CH_3OOH]	$-33 \pm ?$[b]	MM and ab initio calculation[74]
	-33.4 ± 1.2	Δ_fH_{298}[CH_3OO][10] and estimated DH_{298}[CH_3OO-H][75]
	$-31.3 \pm ?$[b]	heat of equilibrium measurement[68]
	-31.4 ± 1.0	group additivity[73]
	-30.9 ± 0.7	CBS/APNO
Δ_fH_{298}[CH_3CH_2OO]	-6.5 ± 2.4	$CH_3CH_2 + O_2 \rightleftarrows CH_3CH_2OO$[12]
	-2.9 ± 1.1	group additivity using DH_{298}[CH_3OO-H] = 88.6 ± 0.5 kcal mol^{-1} [73]
	-6.8 ± 0.7	CBS/APNO
	-6.8 ± 2.3	negative-ion/acidity/CBS[a]
Δ_fH_{298}[CH_3CH_2OOH]	-45 ± 12	static bomb calorimetry[69]
	$-40 \pm ?$[b]	MM and ab initio calculation[74]
	-41.5 ± 1.5	calculation of isodesmic reactions[75]
	-39.4 ± 1.0	group additivity[73]
	-39.5 ± 0.7	CBS/APNO calculation
Δ_fH_{298}[$(CH_3)_3COO$]	$-20.7 \pm ?$[b]	$Br + (CH_3)_3COOH \rightleftarrows (CH_3)_3COO + HBr$[85]
	-24.3 ± 2.2	$(CH_3)_3C + O_2 \rightleftarrows (CH_3)_3COO$[11,12]
	-21.4 ± 1.1	group additivity using DH_{298}[$(CH_3)_3COO-H$] = 88.6 ± 0.5 kcal mol^{-1} [73]
	-25.8 ± 1.2	CBS-Q
	-25.2 ± 2.5	negative-ion/acidity/CBS[a]
	-25.9 ± 2.3	Δ_fH_{298}[$(CH_3)_3COOH$][86,87] from calorimetry and DH_{298}[$(CH_3)_3COO-H$] from Table 4
Δ_fH_{298}[$(CH_3)_3COOH$]	-58.8 ± 1.2	calorimetry[86,87]
	$-56.1 \pm ?$[b]	heat of equilibrium measurement[68]
	-57.9 ± 1.0	group additivity[73]
	-57.3 ± 1.2	CBS-Q

[a] Negative-ion/acidity/CBS refers to the heat of formation of the ROO radical determined in this study using Δ_fH_{298}[ROOH] from CBS/APNO or CBS-Q calculation, DH_{298}(ROO−H) from experiment (Table 4), and Δ_fH_{298}[H] = 52.1028 ± 0.0014 kcal mol^{-1}.[56] [b] Uncertainty not specified.

oxide Δ_fH_{298}[CH_3CH_2OOH] = -41.5 ± 1.5 kcal mol^{-1}. However, since the work of Lay et al.[75] is based on the measurements of Slagle and Gutman[10] (which we would like to verify independently), we will not consider these values for the following discussions but return to them later for comparison.

In the absence of definitive heats of formation for the alkyl hydroperoxides, we have used the generally reliable CBS ab initio electronic structure methods of Petersson and co-workers[36,37] to calculate the following heats of formation: Δ_fH_{298}[HOOH] = -31.7 ± 0.7 kcal mol^{-1}, Δ_fH_{298}[CH_3OOH] = -30.9 ± 0.7 kcal mol^{-1}, Δ_fH_{298}[CH_3CH_2OOH] = -39.5 ± 0.7 kcal mol^{-1}, and Δ_fH_{298}[$(CH_3)_3COOH$] = -57.3 ± 1.2 kcal mol^{-1}. These values show reasonable to very good agreement with most of the experimental and theoretical determinations listed in Table 5. Uncertainties of ± 0.7 and 1.2 kcal mol^{-1} have been recommended for the CBS/APNO and CBS-Q methods, respectively, by comparison of calculated and experimental heats of formation for the G2 test set.[37] In Table 5 we compare the calculated heats of formation of HOOH and $(CH_3)_3COOH$ with the available experimental heats of formation. The calculated values agree within 0.8 and 1.5 kcal mol^{-1} of the respective experimental values. This provides confidence in our calculated heats of formation of CH_3OOH and CH_3CH_2OOH presented above. Combining the calculated heats of formation with our experimental bond enthalpies (Table 4) and Δ_fH_{298}[H] = 52.1028 ± 0.0014 kcal mol^{-1} according to eq 30 gives heats of formation for the methyl, ethyl, and *tert*-butyl peroxyl radicals of Δ_fH_{298}[CH_3OO] = 4.8 ± 1.2 kcal mol^{-1}, Δ_fH_{298}[CH_3CH_2OO] = -6.8 ± 2.3 kcal mol^{-1}, and Δ_fH_{298}[$(CH_3)_3COO$] = -25.2 ± 2.5 kcal mol^{-1}. Therefore, our estimated lower limit for the heat of formation of the methyl peroxyl radical is 3.6 kcal mol^{-1}, which falls just outside the stated uncertainty of Knyazev and Slagle,[12] who obtained Δ_fH_{298}[CH_3OO] = 2.2 ± 1.2 kcal mol^{-1}. Their value was obtained from the experimental observation of the reaction of methyl radical with dioxygen [$CH_3 + O_2 \rightleftarrows CH_3OO$], for which the enthalpy was determined to be $\Delta_{rxn}H_{298} = -32.7 \pm 0.9$ kcal mol^{-1} by measurement of the forward and reverse rate constants. The agreement is, however, excellent for the ethyl and *tert*-butyl peroxyl radicals for which Knyazev and Slagle[12] report heats of formation of Δ_fH_{298}[CH_3CH_2OO] = -6.5 ± 2.5 kcal mol^{-1} and Δ_fH_{298}[$(CH_3)_3COO$] = -24.3 ± 2.2 kcal mol^{-1}, respectively. It is interesting to note that if we combine the Δ_fH_{298}[ROOH] values [where R = CH_3, CH_3CH_2, and $(CH_3)_3C$] derived from group additivity (Table 5)[73] with our experimentally determined bond enthalpies, the resulting heats of formation, Δ_fH_{298}[CH_3OO] = 4.3 ± 1.4 kcal mol^{-1}, Δ_fH_{298}[CH_3CH_2OO] = -6.7 ± 2.4 kcal mol^{-1}, and

(76) Kondo, O.; Benson, S. W. *Int. J. Chem. Kinet.* **1984**, *16*, 949.

Table 6. Experimental Electron Affinities, Acidities, Bond Energies and Term Energies for the Alkyl Peroxyl Radicals, ROO, and Hydroperoxides, ROOH (All Values in kcal mol^{-1})

R	*EA*[ROO]	$\Delta_{acid}H_{298}$[ROOH]	DH_{298}[ROOH]	DH_0[ROOH]	T_0[ROO]
H	24.8 ± 0.1	376.7 ± 0.8	87.9 ± 0.8	86.7 ± 0.8	20.1 ± 0.2
CH_3	26.8 ± 0.1	374.6 ± 1.0	87.8 ± 1.0	86.9 ± 1.0	21.1 ± 0.1
CH_3CH_2	27.3 ± 0.1	371.0 ± 2.2	84.8 ± 2.2	83.9 ± 2.2	21.6 ± 0.1
$(CH_3)_3C$	27.6 ± 0.3	370.2 ± 2.1	84.2 ± 2.1	83.3 ± 2.1	22.3 ± 0.3

$\Delta_fH_{298}[(CH_3)_3COO] = -25.8 \pm 2.4$ kcal mol^{-1}, agree within the stated uncertainty with our "electron affinity/acidity/CBS" results.

Using the electron affinity/acidity/CBS-derived values for $\Delta_fH_{298}[CH_3OO]$, $\Delta_fH_{298}[CH_3CH_2OO]$, and $\Delta_fH_{298}[(CH_3)_3COO]$, it is possible to calculate the enthalpies of the reactions of dioxygen with methyl, ethyl, and *tert*-butyl radicals, respectively. The following heats of formation are employed for the alkyl radicals: $\Delta_fH_{298}[CH_3] = 34.9 \pm 0.3$ kcal mol^{-1}, $\Delta_fH_{298}[CH_3CH_2] = 28.9 \pm 0.4$ kcal mol^{-1}, and $\Delta_fH_{298}[(CH_3)_3C] = 12.3 \pm 0.4$ kcal mol^{-1}.[60] With these auxiliary thermochemical values, we calculate $\Delta_{rxn}H_{298}[CH_3 + O_2 \rightarrow CH_3OO] = -30.1 \pm 1.2$ kcal mol^{-1}, $\Delta_{rxn}H_{298}[CH_3CH_2 + O_2 \rightarrow CH_3CH_2OO] = -35.7 \pm 2.3$ kcal mol^{-1}, and $\Delta_{rxn}H_{298}[(CH_3)_3C + O_2 \rightarrow (CH_3)_3COO] = -37.5 \pm 2.5$ kcal mol^{-1}.[77] Our result for the reaction enthalpy of $[CH_3 + O_2]$ falls just outside the uncertainties reported by Knyazev and Slagle[12] (vide supra); however, the values for $[CH_3CH_2 + O_2]$ and $[(CH_3)_3C + O_2]$ fall within the uncertainties of $\Delta_{rxn}H_{298}[CH_3CH_2 + O_2] = -35.5 \pm 2.0$ kcal mol^{-1} and $\Delta_{rxn}H_{298}[(CH_3)_3C + O_2] = -36.5 \pm 1.8$ kcal mol^{-1} reported by these authors. This is significant agreement on the exothermicity of several important gas-phase reactions (reaction 8).

These experimental reaction enthalpies are in disagreement with recent high-level computational studies,[8,9] which suggest that the reaction is less exothermic with heats of reaction of just -31.5 or -30.1 kcal mol^{-1} for $\Delta_{rxn}H_{298}[CH_3CH_2 + O_2]$. It should be reiterated that our value for the reaction enthalpy is not completely "experimental", since it depends in part on the computationally determined heat of formation of ethyl hydroperoxide. Comparing this value with other literature numbers (cf. Table 5) suggests that this is an upper limit and using any of the other cited values for deducing the heat of formation of the ethyl peroxyl radical would generate a smaller value and consequently make reaction 8 more exothermic.

Table 6 summarizes the physical properties of the peroxyl radicals (ROO) and their parent hydroperoxides (ROOH) as the alkyl group increases in size. These data reveal a number of trends that allow us to make some useful predictions about the physical properties of other, larger alkyl hydroperoxides and alkyl peroxyl radicals. The electron affinities of the peroxyl radicals (ROO) increase slightly as the substituent increases in size. This trend is subtle, however, with all electron affinities falling within 0.1 eV. Thus, we anticipate that alkyl peroxyl radicals, whether linear or branched structures, will have $EA(C_nH_{2n+1}OO) = 1.2 \pm 0.1$ eV. There is also a trend toward decreasing values of $\Delta_{acid}H_{298}$ with increasing length of the alkyl chain. Table 6 indicates that HOOH is the weakest acid of this series, followed by CH_3OOH, CH_3CH_2OOH, and $(CH_3)_3COOH$, which is the strongest acid. This trend is analogous to the behavior of the acidity of water and related, simple alkyl alcohols.[78] Excluding HOOH, the alkyl hydroperoxides demonstrate a decreasing bond enthalpy (DH_{298}[ROO−H]) with increasing R group size. This is clear when comparing $DH_{298}[CH_3OO-H]$ and $DH_{298}[CH_3CH_2OO-H]$, but the difference between $DH_{298}[CH_3CH_2OO-H]$ and $DH_{298}[(CH_3)_3COO-H]$ is small compared with the stated uncertainties. However, although the absolute uncertainties for $DH_{298}[CH_3CH_2OO-H]$ and $DH_{298}[(CH_3)_3COO-H]$ are large, it must be remembered that the relative uncertainties are much smaller ($\cong$0.4 kcal mol^{-1}, see preceding discussion on gas-phase acidity), and thus the slight decrease in bond enthalpy is meaningful. This trend suggests that other alkyl hydroperoxides will have bond enthalpies similar to that of ethyl hydroperoxide ($DH_{298}[C_nH_{2n+1}OOH] \cong 85 \pm 2$ kcal mol^{-1}). Earlier authors[73] have suggested 88.6 ± 0.5 kcal mol^{-1} as a "universal" DH_{298}[ROO−H] bond enthalpy; Table 6 indicates that 85 ± 2 kcal mol^{-1} is a more useful, conservative estimate.

Acknowledgment. S.J.B., M.R.N., and G.B.E. are pleased to acknowledge support by the Chemical Physics Program, United States Department of Energy (DE-FG02-87ER13695); G.B.E. is a Fellow of the J. S. Guggenheim Foundation. W.C.L. is pleased to ackowledge support from the National Science Foundation (CHE 9703486). V.M.B. and S.K. gratefully acknowledge support from the National Science Foundation (CHE 9734867). M.O. is pleased to acknowledge JILA for the award of a Visiting Fellowship and the National Science Foundation (grant CHE 9700610). The GAUSSIAN98 calculations were carried out in part with a cluster of RSC-6000 digital computers supported by NSF (CHE 9412767) and in part using the facilities of the National Center for Supercomputing Application (CE980028N). We thank Prof. Tarek Sammakia for advice and assistance with the preparation of the methyl and ethyl hydroperoxides and Prof. Chuck DePuy for useful discussions.

Supporting Information Available: Two tables giving molecular geometries, rotational constants, and harmonic frequencies calculated at the B3LYP/aug-cc-pVDZ level of theory for ROO^-, ROO ($\tilde{X}$ and $\tilde{A}$), and ROOH (where R = CH_3, CD_3, and CH_3CH_2) (PDF). This material is available free of charge via the Internet at http://pubs.acs.org.

JA010942J

(77) These data suggest an increase in the C−O bond enthalpy for alkyl peroxyl radicals, DH_{298}[R−OO], with increasing alkyl group size (i.e., $DH_{298}[CH_3-OO] = 30.1 \pm 1.1$ kcal mol^{-1}, $DH_{298}[CH_3CH_2-OO] = 35.7 \pm 2.2$ kcal mol^{-1}, and $DH_{298}[(CH_3)_3C-OO] = 37.5 \pm 2.4$ kcal mol^{-1}). This trend is analogous to that observed for alcohols, where the estimated C−O bond enthalpies also increase with the size of the alkyl substituent (i.e., $DH_{298}[CH_3-OH] = 91.9 \pm 0.3$ kcal mol^{-1}, $DH_{298}[CH_3CH_2-OH] = 93.9 \pm 0.4$ kcal mol^{-1}, and $DH_{298}[(CH_3)_3C-OH] = 95.9 \pm 0.4$ kcal mol^{-1}).

(78) Brauman, J. I.; Blair, L. K. *J. Am. Chem. Soc.* **1970**, *92*, 5986.
(79) Oakes, J. M.; Harding, L. B.; Ellison, G. B. *J. Chem. Phys.* **1985**, *83*, 5400.
(80) Gurvich, L. V.; Veyts, I. V.; Alcock, C. B.; Iorsish, V. S. *Thermodynamic Properties of Individual Substances*, 4th ed.; Hemisphere: New York, 1991.
(81) Hills, A. J.; Howard, C. J. *J. Chem. Phys.* **1984**, *81*, 4458.
(82) Golden, D. M.; Bierbaum, V. M.; Howard, C. J. *J. Phys. Chem.* **1990**, *94*, 5413.
(83) Khachatryan, L. A.; Niazyan, O. M.; Mantashyan, A. A.; Vedeneev, V. I.; Teitelboim, M. A. *Int. J. Chem. Kinet.* **1982**, *14*, 1231.
(84) Kondo, O.; Benson, S. W. *J. Phys. Chem.* **1984**, *88*, 6675.
(85) Heneghan, S. P.; Benson, S. W. *Int. J. Chem. Kinet.* **1983**, *15*, 815.
(86) Kozlov, N. A.; Raniovich, I. B. *Tr. Khim. Khim. Tekhnol.* **1964**, *2*, 189.
(87) Kozlov, N. A.; Raniovich, I. B. *Chem. Abstr.* **1965**, *63*, 6387; **1965**, *63*, 6387.